Kinetics Study on Catalytic Degradation of Corn cob using CaO/γ Al_2O_3 Catalyst

By

Mesay Teshome Adugna

Thesis Paper Submitted to Chemical Engineering

School of Mechanical, Chemical and Materials Engineering

Presented in Partial Fulfillment of the Requirements for the Award of the Degree of Masters of Science in Chemical Engineering (Specialization in Process Engineering)

Office of Graduate Studies

Adama Science and Technology University

Adama, Ethiopia

March, 2021

Kinetics Study on Catalytic Degradation of Corn cob using CaO/γ-Al_2O_3 catalyst

By

Mesay Teshome Adugna

Advisor Name: Zelalem Tumsa (Ph.D.)

Co-Advisor Name: Melaku Tesfaye (Ph.D.)

Thesis Paper Submitted to Chemical Engineering

School of Mechanical, Chemical and Materials Engineering

Presented in Partial Fulfillment of the Requirements for the Award of the Degree of Masters of Science in Chemical Engineering

(Specialization in Process Engineering)

Office of Graduate Studies

Adama Science and Technology University

Adama, Ethiopia

March, 2021

THESIS APPROVAL SHEET

We, the undersigned, members of the Board of Examiners of the final open defense by Mesay Teshome adugna have read and evaluated his/her thesis entitled " kinetic study of catalytic degradation of corn cob using $CaO/\gamma\text{-}Al_2O_3$ catalyst" and examined the candidate. This is therefore, to certify that the thesis has been accepted in partial fulfillment of the requirement of the Degree of Master of Science in Chemical engineering.

Advisor	Signature	Date
Co-Advisor	Signature	Date
Chairperson	Signature	Date
External Examiner	Signature	Date
Internal Examiner	Signature	Date
Head of Department	Signature	Date
School Dean	Signature	Date
Post Graduate Dean	Signature	Date

DECLARATION

Hereby declare that this MSc thesis entitled "kinetic study of catalytic degradation of corn cob using $CaO/\gamma\text{-}Al_2O_3$ catalyst "in partial fulfillment of the requirements for the award of the Degree of Masters of Science in Chemical engineering is my original work carried out from February 2020 to March 2021 under the supervision of Dr. Zelalem Tumsa and Dr. Melaku Tesfaye, Department of Chemical engineering, Adama Science and Technology University, Ethiopia. It has not been presented for a degree in any other university, and all sources of material used for this thesis have been duly acknowledged.

Name Signature Date

Mesay Teshome

_____ _____ _____

Candidate

This MSc/ MA Thesis have been submitted for examination with my approval as thesis advisor/ dissertation Supervisor.

Name Signature Date

Dr. Zelalem Tumsa

_____ _____ _____

Advisor

Dr. Melaku Tesfaye

_____ _____ _____

Co-Advisor

DEDICATION

I dedicate this research to my beloved mother Fentansh Kinda, my father Teshome Adugna and all my brothers and sisters. Also, I am pleased to research in loving memory of my friend Maru Alemayehu, who died in December 2006 E C.

ACKNOWLEDGEMENT

First and foremost, glory to the almighty God, for protecting and giving courage to me to complete my study and in every step of my life.

I would like to express my sincere gratitude to my advisors Dr. Zelalem Tumsa and Dr. Melaku Tesfaye for their continuous guidance, encouragement and support in making this research possible. .

I would like to express my deep gratitude to Bahir Dar University, who gave me approval for experimenting in their laboratory and also Mr. Alebel Abebaw, who helped me during experimental work.

I wish to express my honest gratitude to my family for their great support and understanding while working on this thesis and through all my graduate studies.

I would like to acknowledge and appreciate all of my friends who have played a valuable role in my work by sharing supportive materials, data, information and ideas.

Lastly, I have to give special thanks to Adama Science and Technology University for financial support

Table of Contents

LIST OF FIGURES

LIST OF TABLES

LIST OF SYMBOLS

A	Pre- exponential frequency
E	Activation energy
f(α)	Reaction model function
g(α)	Conversion function
k(T)	Cate constant
M	Mass at a time
m_0	Initial mass
Mba	Mass of benzoic acid
M_{dried}	Weight of corn cob material
$M_{initial}$	Before dry base of corn cob
Q_{fuse}	Heat attributed to the cotton thread
Q_{ign}	Heat attributed to the Nichrome ignition wire
Q_{vba}	Gross calorific value of benzoic acid
R	Universal gas constant
T	Time
T	Absolute temperature
W	Normalized mass
W_{ash}	Ash content
Wcc	Weight of corn cob
W_z	Normalized final mass
Wo	Normalized initial mass
Wto	Weight of initial mass of cut-off sample
Wα	Weight of cut-off sample at a particular temperature
A	Degree of conversion
B	Heating rate
ΔT	Corrected temperature rise of the calorimeter vessel

LIST OF ABBREVIATION

%ACC	Percentage ash content of corn cob
%FCCC	Percentage fixed carbon content of corn cob
%MCC	Percentage of moisture content
%VM	Percentages of volatiles
CC	Corn Cob
CC1	Gamma alumna support
CC2	10% calcium oxide loaded on Gamma alumna support
CC3	20% calcium oxide loaded on Gamma alumna support
CC4	30% calcium oxide loaded on Gamma alumna support
CC5	40% calcium oxide loaded on Gamma alumna support
CC6	50% calcium oxide loaded on Gamma alumna support
CH_4	Methane
CO	Carbon monoxide
CO_2	Carbon dioxide
FTIR	Fourier transforms infrared
FWO	Ozawa-Flynn-Wall
H_2	Hydrogen
HHV	Higher Heating Valve
K_2CO_3	Potassium carbonate
KAS	Kissinger- Akahira- Sunose
KOH	Potassium hydro oxide
LHV	Lower Heating Valve
MgO	Magnesium oxide
MSW	Municipal solid wastes
Na_2CO_3	Sodium carbonate
Na_2O	Sodium oxide
NaCl	Sodium chloride
NaOH	Sodium hydro oxide
SEM	Scanning Electron Microscopy
TGA	Thermo-Gravimetric Analysis
XRD	X-ray diffraction
γ-Al_2O_3	Gamma alumna

ABSTRACT

Biomass is the promising renewable energy sources which can be converted into liquid and gaseous fuels through various technologies. Thermochemical conversion of biomass is a common technology for the conversion of biomass into fuels .In this work, a thermo gravimetric analysis of Corn cob in the presence of CaO/ γ-Al_2O_3 catalyst is conducted. Pyrolysis experiments of corn cob with CaO/γ-Al_2O_3 catalyst with the main aim of development of the kinetic modeling for the catalytic decomposition process. The kinetics study of catalytic cracking of corn cob using CaO/γ-Al_2O_3 catalyst was investigated over temperature range 25-800°C. The catalyst was prepared from Aluminum nitrate nonahydrate, urea, and $CaCO_3$ using impregnation method followed by activation at 700°C for 4:30hr in the furnace. The catalyst was characterized with X-ray diffraction (XRD), Fourier transform infrared spectroscopy (FTIR) and Thermo gravimetric analysis (TGA) and Scanning electron microscopy (SEM). Thermal analysis was carried out for all samples using TGA in order to study the catalytic performance of all CaO/γ-Al_2O_3 on decomposition of corn cob in the process of pyrolysis. The obtained results were shown on TG and DTG graphs. The decomposition of all samples containing 0, 10, 20, 30, 40 and 50 wt% CaO/γ-Al_2O_3 catalysts were compared to each other and to the reference sample (corn cob). The results showed best decomposition rate was observed when 10 wt% CaO loaded on γ-Al_2O_3 used as a catalyst. Kinetic models were investigated based on weight loss dependence to temperature in the pyrolysis process of corn cob with 10wt% CaO/γ-Al_2O_3 containing sample. The decomposition stage was divided into two different zones to attain the well-fitted reaction model with high coefficient of determination (R^2) using linear regressions. The activation energy (Ea) and correlation coefficient (R^2) profiles revealed that the kinetic parameters calculated using the Flynn–Wall–Ozawa and Kissinger–Akahira–Sunose method. The values from the Flynn–Wall–Ozawa methods were comparable, although gave higher R^2 values. The Eα values gradually reduced from 165.87kJ/mol to 129.186kJ/mol and 177.18 to 96.7kJ/mol with an increase in from 0.3 to 0.5 and 0.51 to 0.8 respectively. The model-fitting method of Coats–Redfern was used to predict the possible reaction mechanism, for which the F6.5 and F4 model resulted in comparable Eα values to those obtained from the Flynn–Wall– Ozawa method. The pre-exponential factors (lnA) were calculated based on the F6.5 and F4 reaction model and the Flynn–Wall–Ozawa method, and fell in the range of 17.6–13.26 $min^{-1}$and 17.63-8.95 min^{-1} with α increasing from 0.3 to 0.5 and 0.51-0.9 respectively. The study of the kinetic compensation effect confirmed that a compensation effect existed between Ea and lnA during the corn cob pyrolysis. Results obtained in this thesis may be the base for wide range of scientific studies in the future to examine the catalytic degradation nature of 10 wt% CaO/γ-Al_2O_3 and further analysis of catalysts obtained in this work in the synthesis of bio-oil from corn cob and different biomass feedstock

Key Words: biomass, corn cob, bio-oil, TGA, FWO and KAS

CHAPTER ONE

1. INTRODUCTION

1.1. Background of study

In this 21st century, energy demand is continually increasing with the rise in population. The majority of energy demand is currently fulfilled by fossil fuels and partially by renewable energy. Energy consumption in the developed and developing worlds is greatly different. The developed world predominantly consumes energy from coal, petroleum and natural gas, and to some extent, renewable energy sources[1]. In contrast, developing world is still largely dependent on biomass domestic energy fuel sources that typical burn in traditional stove. However, environmental issue such as global warming and air pollution happen due to fossil fuel consumption, growing energy demand and depletion of fossil fuel have stimulated the demand for renewable fuel [2].

Biomass is all organic material that is available on renewable or recurring basis, and such thing as agriculture corps and waste, wood and wood waste, animal waste, aquatic plant, and organic fractions of municipal waste. Lignocellulosic biomass are mainly composed of macromolecular (cellulose, hemicellulose and lignin) together with smaller amount of low molecular weight substances extracted and inorganic (salt or minerals). There are a number of biomass sources being considered as potential sources of fuel and chemical feedstocks in Ethiopia [3], [4].

In Ethiopia, among grain, corn has got the widest field for planting after teff, wheat and barley [5]. Corn is an important plant as human nourishment, animal folder and industrial material. Corn cob is by product of corn for every 100 kg of corn grain approximately 20 kg of corn cob are produced. However, corn cob is still discharged in productive ways, usually burnt which result in irreparable harm to the environment, which is directly related to air pollution. The composition of corn cob contains valuable materials 40-60% cellulose, 15-30% hemicellulose and 15-25% lignin. It was thought that corn cob could be utilized as agriculture by product renewable energy sources [6].

Conversion of biomass into energy sources (electricity and biofuel) has been practiced from long time. Direct combustion of biomass, historically, has been the primary sources of energy throughout the world, for residential activity and small industry in rural area. Unforturtly, direct burning of loose biomass in conventional grate is always associated with low energy efficiency and contributes adverse impact to the environment, particularly

the air quality. Modern technology which offer clean and efficient energy conversion, is required to improve the attractiveness of biomass utilization as energy sources[7].

Biomass can be converted mainly through the necessary biochemical and thermochemical processes. Thermochemical processes required relatively high temperature and sometimes high pressures to decompose biomass into the smaller molecular weight compound that can convert into hydrocarbon, alcohol or aromatic via the catalytic processes. Thermochemical methods such as gasification, liquefaction, pyrolysis, torrefaction and combustion, are usually preferred over biochemical methods for energy production[8].

Pyrolysis is a process, where organics materials are exposed to thermal treatment in absences of an oxidizing agent, resulting in bio-char, bio-oil, gases(CO, CO_2,CH_4, and H_2)[9]. The catalytic pyrolysis of biomass is the proven way that can be used to improve the cracking reaction and quality of products. Basically this process involves the biomass thermal decomposition stages as occur in thermogravimetric analysis, but with the presences of the catalyst it can be used to lower the pyrolysis temperature[10].

The reaction kinetics of biomass is usually studied by thermogravimetric analysis (TGA), an experimental technique giving mass-loss data as function of time and temperature. The kinetics models derived from such data can be used to describe the overall conversion and if vapors are condensed, the product distribution volatiles and gas. The method used to derive or develop kinetics parameter from experimental thermal analysis data can be categorized into modeling-fitting and model-free methods[11], [12].

The apparent activation energy can be calculated using isoconversional methods accurately without prior knowledge of reaction model order. However, biomass pyrolysis is a complex process involving many secondary reactions. It is reported that isoconversional methods are suitable only when one-step reactions are considered[13]. The model fitting methods are used to determine kinetic parameters and reaction mechanism for complex biomass decomposition. It has been determined by identifying model functions which present thermal decomposition behavior of complex. For lignocellulosic biomass, decomposition includes more than one reaction involving parallel reactions of the three components commonly present[14]. Several researchers have studied the pyrolytic behavior and kinetics of biomass using thermogravimetry analysis[15].

The kinetic parameters calculated from the order-based model of solid-state reactions resulted in significant deviations. Hence, integral methods of Kissinger-Akahira-Sunose

and Flynn-Wall-Ozawa have been used more in the kinetic analysis of biomass now days. The activation energy can be calculated from TGA and DTG curve data based on model-effects. Therefore, model-free model error result from kinetic analysis through Arrhenius parameter estimation can be avoided [16]. The pre-exponential factor is the pre-exponential constant in the Arrhenius equation an empirical relationship between temperature and rate coefficient. Presently, thermal degradation of lignocellulosic biomass is extensively studied using model-free methods.

The model-fitting method is considered as reaction mechanism model where the kinetic parameters calculated using linear regression to fit the experimental data. Kinetic parameters represented by the integral form g (α) are based on the pseudo-reaction schemes. In addition, temperature and conversion vary simultaneously with time; therefore, it is difficult to obtain a unique solution. The activation energy estimated by model-fitting methods is an implicit function of (temperature and conversion). However, the activation energy represents the average value of the overall pyrolysis process [17].

The derived values are assumed to be invariant to the reaction mechanism and kinetics of process which vary with temperature and extent of conversion. Hence, the isoconversional methods have provided weightage over model-based schemes to overcome drawbacks of inconsistent values [18], [19]. One of model-fitting method Coats Redfern is used in evaluating kinetics parameters this method derives Arrhenius parameters from a single heating rate. This scheme is highly inaccurate. It is suggested that the kinetic analysis should not be based on the single heating rate. Furthermore, thermal decomposition of biomass indicates that the results obtained from Coats-Redfern are highly incoherent as compared to model-free scheme [20].

This study aims to investigate the kinetics of catalytic thermal decomposition of corn cob using thermogravimetric analysis. It also focuses on synthesis and characterization of heterogeneous metal oxides ($CaO/\gamma\text{-}Al_2O_3$) which can be used to enhance the catalytic pyrolysis of corn cob.

1.2. Statement of problem

The thermal pyrolysis requires high temperatures, which often results in products with low quality, making this process unfeasible (the value activation energy increases it's also a high amount of pyrolysis reactor cost). This occurs because the uncatalyzed thermal degradation gives raise to low molecular weight substances, however, in a very wide range

of products. This method can be improved by the addition of catalysts, which will reduce the temperature and reaction time and allow the production of hydrocarbons with a higher added value, such as fuel oils and petrochemical feedstocks [21]–[23]. That is, the use of catalysts gives an added value to the pyrolysis and cracking efficiency of these catalysts depends both on its chemical and physical characteristics. These particular properties promote the breaking of C-C bonds and determine the length of the chains of the products obtained[24].

Ethiopia is one of the developing countries in the world with quite many rural settlements that are associated with energy challenges because of the difficulties in extending the national electricity grid to these settlements. Therefore, the energy needs of these remote areas have to be met 94% of biomass (off-grid technologies) is mostly for traditional cooking and heating. This traditional use of biomass implies very low conversion efficiencies, around 10% to 20%, and health damage issues through air pollution[25]. Therefore, the energy needs of these remote areas have to be met by off-grid technology that is economically viable and sustainable. There are four different types of off-grid power generation methods, namely, the solar, wind, hydropower and biomass power generation. Because of the high cost associated with the first three, power generation from biomass happens to be the most convenient and yet efficient method of providing energy to a remote settlement [26].

In Ethiopia farmer produces many agricultural, plantation, and forestry residues which could be converted into valuable fuels and chemical products. These waste materials have not or a little economic value, often present as a disposal problem. Fossil fuel, the dominant source of energy today modern civilization has been a significant negative impact on depletion, global climate change and other environmental concern. The major concerns of replacing fossil fuel into biomass energy is to reduce environmental and energy crisis by the conversion of corn cob into useful liquid fuel via catalytic pyrolysis[27].

1.3. General objective

The general objective of this thesis is to study/investigates of catalytic degradation of corn cob using $CaO/\gamma\text{-}Al_2O_3$ catalyst.

1.3.1. Specific objective

The specific objective are:-

- To characterize proximate, ultimate analysis and heating value of corn cob.
- To synthesize and characterize CaO/γ- Al_2O_3 catalyst.
- To study the use of CaO/γ- Al_2O_3 catalyst to enhance thermal degradation of corn cob.
- To investigate the main operating parameters (catalyst loading and heating rate) of catalytic degradation of corn cob.
- To study the kinetics of corn cob in the presences of CaO/γ- Al_2O_3 catalyst.

1.4. Research question

After studying the literature review and identifying the knowledge gap a research question was framed to focus the project. The research questions are as follows:

1. Is it possible to synthesize a heterogeneous metal oxide with better performance for efficient catalytic cracking of corn cob?
2. How does a CaO/γ-Al_2O_3 catalyst affects the thermal decomposition of corn cob?
3. How to develop the decomposition kinetics of corn cob with and without the newly developed CaO/γ- Al_2O_3 catalyst that fit the experiment?
4. How the operating parameters affect the decomposition kinetics and what is the optimum catalyst loading?

1.5. Significance of study

The current world dependency on fossil fuel produces concerns over energy security and global warning. One way to mitigate this is to promote the use of alternative fuels such as biomass. Biomasses have received worldwide interest due to its great potential to substitute fossil fuels for production of electricity, fuels, and chemicals. Biomass has several significant advantages, including its abundance, renewability, and carbon-neutrality as well as low sulfur content.

Forestry and agricultural waste represent a good opportunity in this sense as a by-product from forest and agriculture management with not a widespread usage. To obtain energy out of the forestry and agricultural waste, pyrolysis is an alternative to direct combustion due to the recovery of solid and liquid materials which can be readily stored and transported. The liquid material known as bio-oil is advantageous because its volumetric energy density is 4-5 times higher (or even more) than the solid biomass[28].

Catalytic degradation of biomass uses a suitable catalyst to carry out the cracking reaction. The presences of catalyst can promote the decomposition reaction at lower temperature

with lower energy consumption, reduce equipment and energy costs, increase the yield of products with higher added value, increase the process selectively, faster cracking reactions, lead to smaller volumes and inhibiting the formation of undesirable products[29] - [30].

In order to design industrial reactor, as well as to obtain important empirical parameters for process modeling and controlling the kinetics involved in biomass pyrolysis should be well understood. This not only allow the estimation of kinetic parameters, but also the simulations beyond the temperature range [31].

1.6. Scope of study

The research work generally covers:-

- Corn cob preparation and characterization.
- Synthesis and characterization of heterogeneous ($CaO/\gamma\text{-}Al_2O_3$) catalyst.
- Thermogravimetric analysis of corn cob at different heating rate and catalyst loading.
- Predict the kinetic study of catalytic thermal degradation of corn cob.

1.7. Organization of study

This thesis is organized into five chapters

Chapter 1:- The first chapter present background study, statement of problem, objective, research question, significances of study and scope of research.

Chapter 2: discuss extensive literature reviews related to biomass, factor affecting biomass, composition of biomass, corn cob pretreatment of corn cob, thermal decomposition kinetics, effect of operating parameter and catalytic pyrolysis of biomass using TGA.

Chapter 3:- The third chapter describes material and method used to prepare corn cob and catalysts, characterize corn cob and catalysts, study the catalytic degradation of corn cob, effect of catalyst loading and heating rate, select reaction models and predicts the kinetics parameters.

Chapter 4:- The results obtained and discussions are presented in this chapter. Discuses about characterization results of corn cob and catalyst, best catalyst screening of catalytic degradation of corn cob, effect of catalyst loading and heating rate, reaction mechanism and determination of kinetics parameters using different kinetic model.

Chapter 5:- Last chapter discussed about conclusion and recommendation.

CHAPTER TWO

2. LITERATURE REVIEW

This chapter provides an extensive review on biomass and catalyst selection and catalytically degradation of biomass. The literature review part of this Thesis consists of two sections. The first section is a review on biomass, factor affecting biomass, composition of biomass, corn cob and pretreatment of corn cob. The second section is a review on biomass conversion process (pyrolysis and mechanism pyrolysis process), thermal decomposition kinetics (model fitting and free) and effect of operating parameter (particle size, heating rate and catalyst loading), catalyst and support materials (acid and basic metal oxide catalyst).

2.1. Biomass

Biomass can be used to produce renewable electricity, thermal energy, or transportation fuels. Biomass is organic material resulting from living, or recently living organism. Most often it refers to a plant or plant-based materials which are precisely called lignocellulosic. Biomass is carbon based and comprised of a mixture of organic molecules containing hydrogen, oxygen, nitrogen and also small quantities of other atoms, including heavy metals, alkaline earth and alkali metal [32]. The resources of biomass include various natural and derived materials such as agricultural crops and residues, forest wood and leaf residues, municipal solid wastes, forest and mill residues, animal residues, and sewage [33].

On the other hand, biomass can be considered a natural form of solar energy and it is the oldest source of renewable energy known by humankind. Historically the most common way of treating biomass has been by direct combustion converting it to heat to meet the needs of heating, cooking food, steam treatment technologies [34]. There are several ways to produce energy from biomass, including burning biomass to generate heat or run steam turbines that produce electricity, burning biomass to produce heat in thermal systems (when combined with electricity generation, it's called "combined heat and power"), turning feedstock's into liquid biofuels, and harvesting gas from landfills or anaerobic digesters [33], [35]. The main advantage of biomass as an energy vector compared to fossil fuels lies in that its use has a net zero balance of carbon dioxide emissions, also called

closed carbon loop, since the CO_2 emitted during the pyrolysis is counterbalanced by the CO_2 consumed by the plant itself during its growth [36].

Some important additional advantages of the substitution of fossil fuels for biomass are listed below:

- Biomass is not a finite material, but a renewable one.
- It promotes the development and efficiency of the agricultural and forestry sector, contributing to the creation of employment in rural areas, and providing a delocalized energy network, thus avoiding depopulation of these areas.
- The risks of forest fires and insect plagues caused by the rotting of forest residues would be reduced.
- The use of agricultural waste would avoid its burning in the fields.
- The economic and logistic independence from fluctuation in prices and production of fuels from abroad could be achieved.

2.2. Lignocellulosic biomass constituents

A Lignocellulosic biomass are mainly composed of macromolecular substances (cellulose, hemicellulose and lignin) together with amounts of low molecular weight substances such as extractives and inorganics (salt or minerals) [31].

Cellulose is the most common form of carbon in biomass accounting for 35%-60% by weight of biomass depends on the biomass source. It is a complex sugar polymer, or polysaccharide, made from the six-carbon sugar, glucose [37]. Cellulose is usually represented by ($C_6H_{1-+-0}O_5$) n, and the polymerization degree of the long polysaccharide chain approximately 10,000, resulting in a high molecular weight (>500,000). Cellulose is formed by the β-1, 4 glycosidic linkages of D-glucopyranose units [9]. The chemical structure of cellulose chains allows forming strong intra and intermolecular hydrogen bonds due to the oriented hydroxyl groups. Micro and macro fibrils are formed as a result of the hydrogen bonding network and interact with the hemicellulose fraction.

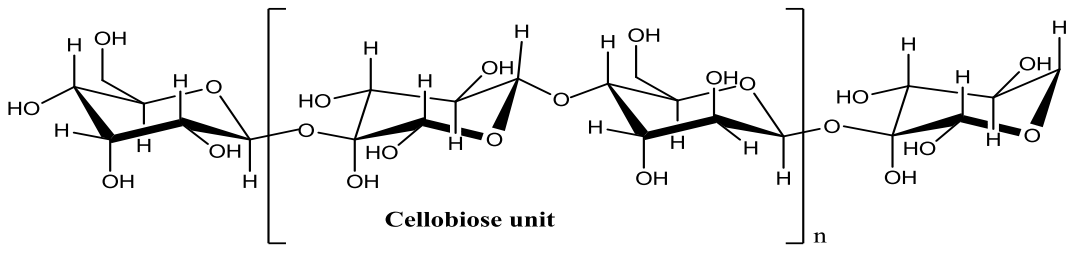

Figure 2.1:- Chemical structure of cellulose [38].

Hemicellulose is a major source of carbon in biomass at levels of between 20-35% by weight. It is a complex polysaccharide made from a variety of five and six carbon sugars. The structure and composition of hemicelluloses differ for different types of biomass. Most of the hemicelluloses contain some simple sugar residues like D-glucose, D-xylose, D-galactose, D-mannose, D-glucurnoic acid and D-ababinose (Shurong Wanga,*, Gongxin Daia,Haiping Yangb, 2017). Cellulose and hemicelluloses are converted into bio-oil than other product at specified operating parameters [39].

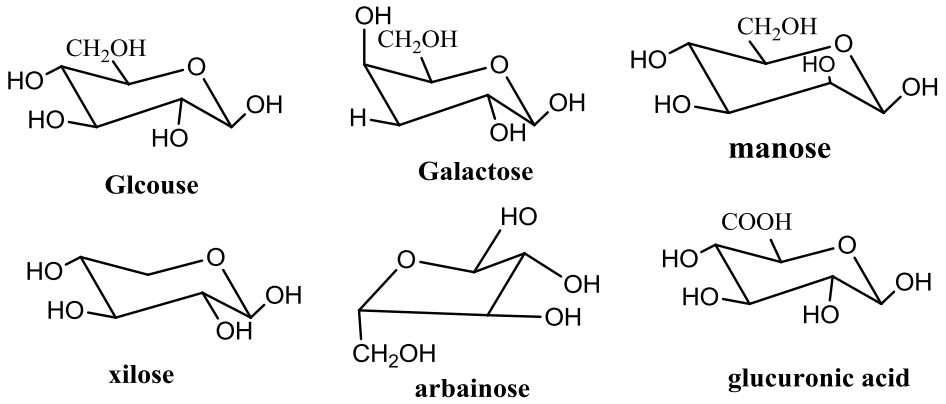

Figure 2.2:- Main components of hemicellulose[40].

Lignin is a complex polymer which provides structural integrity in plants. It makes up 10% to 25% by weight of the biomass. It remains as residual material after the sugars in the biomass have been converted. It contain lot of energy and can be burn to produce steam and electricity for biochemical biomass processing[41].

Lignin is an amorphous polymer formed by randomly cross-linked phenyl propanoid units that connect hemicellulose, cellulose through hydrogen bond and covalent linkages which provides structural rigidity to lignocellulosic matrix. There are mono-lignol monomers which, methoxylated to various degrees (sinapyl alcohol, coniferyl alcohol and p-coumaryl alcohol). Lignin can be used as a low- value heating fuel binder and dispersant. Lignin yields larger proportion of solid char [42]

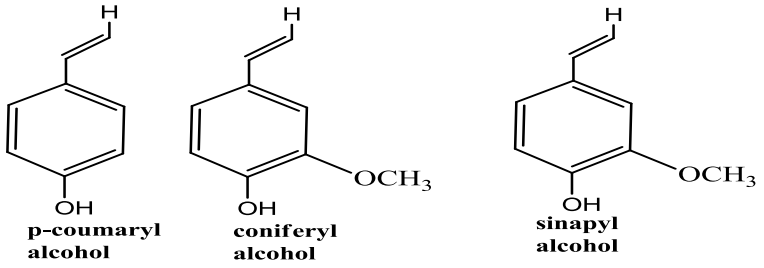

Figure 2.3:- Main components of lignin[40].

Biomass contains a very small amount of inorganic minerals, which are primarily composed of potassium, calcium, sodium, magnesium, silicon, phosphorus and sulfur, etc. Trace amount of aluminum, titanium, vanadium, manganese, iron, cobalt, nickel, cobalt, nickel, copper, nickel, zinc, molybdenum, and other heavy metals may also be present in biomass [27].

Organic extractives in lignocellulosic biomass refer to the non-structural materials that can be extracted by solvents (e.g., water, ethanol, acetone, benzene and toluene), such as fatty acids, simple sugars, waxes and stereols[40].

Table 2.1:- The content of cellulose, hemicellulose, and lignin in common agricultural residues and wastes source[43].

Lignocellulosic materials	Cellulose (%)	Hemicellulose (%)	Lignin (%)
Switch grass	45	31.5	12
Swine waste	6.0	28	Na
Nut shells	25-30	25-30	30-40
Corn cobs	45	35	15
Grasses	25-40	35-50	10-30
Wheat straw	30	50	15
Leaves	15-20	80-85	0
Cotton seed hair	80-95	5-20	0
Newspaper	40-55	25-40	18-30
Waste water solids	8-15	Na	Na
Solid cattle manure	1.6-4.7	1.4-3.3	2.7-5.7
Hardwood stems	40-55	24-40	18-25
Softwood stems	45-50	5-35	25-35
Rice straw	35-45	18-25	10-25

2.3. Corn cob

Corn cob is biomass feedstock with direct potential as energy resources that can be used in pyrolysis systems for energy production. It has a number of advantages over other biomass feedstocks including its dense and uniform nature as well as its increased energy content and its low sulfur and nitrogen concentration. Corn cob consists of the residue left from removing the maize grains from the cobs during harvesting. Cob makes up about 20 % of the yield of corn residue shows in in Table 2.2: corn cob can also contain other leaves and the grain part of harvest corn has higher water content than the corn Stover after harvest

[44]. The separation of the stalks, husks and leaves from the corn cob is achieved by passing a stream of air through the corn plant residue with the lighter stalks, husks and leaves being discharged to the ground with the cobs being collected in storage. Corn cobs are becoming important feedstocks for ethanol and pyrolysis plant. They have more consistent density and ash content than corn Stover [45].

Table 2.2:- Dry matter distribution in corn residues [6].

Corn residue	wt. % of residue
Stalk	50
Leaf	20
Cob	20
Husk	10

2.3.1. Corn cob in Ethiopia

Corn, which was originated from South American and first introduced in Ethiopia in the 16 to 17th century[46]. It is classified as one of warm weather cereal crop and widely cultivated at altitudes ranging from 1500-2200 meter above sea level of Western, South western, and Southern parts of the country. Ethiopia is among major corn producers in Sub Saharan African countries; where smallholder farmers control the major portion of production. Corn is widely grown in Ethiopia only three region states contribute to 94% of total annual production. These regions are Oromia, Amhara, and SNNP. According to a five-year (2003/04-2008/09) CSA data, the share of Oromia region was on the average 60% of the total corn production in country. This was followed by Amhara with 21.67% and SNNP with 12.55%. Thus, the trend of national corn production was entirely dependent on the production of field of the three regions. It accounts for about 10% of the area 12% of the production of the region. Maize yield levels are slightly above the region average about 1.7 metric tons/ha for the whole region[47]. The production capacity of corn cobs depend on the production of corn. Corn cob is essential by product for 100kg of corn grain approximately 20kg of corn cobs are produced[48].

Table 2.3:- Regional corn production statistical tables[5].

Region	Production (in quintals)
Oromia	46,767,440.66
Amhara	17,812,032.42
SNNP	11,969,670.78
Benishangul-Gumuz	2,033,750.51
Tigray	1,590,561.25
Somali	574,831.11
Afar	138,009.12
Gambela	125,827.55
Harari	33,827.52
Dire Dawa	6,296.35
Total	83,958,872.44

2.4. Pretreatment of corn cob

The corn cob feedstock usually requires some form of pretreatment before its pyrolysis. The aim of the pretreatment is to change or even destruct the lignocellulosic structure so that the pyrolysis efficiency can be enhanced. Corn cob pretreatment methods can be classified into four (physical, chemical, biological and thermal pretreatment). During thermal degradation from corn cob is treated by thermal and physical pretreatment [3].

Physical Pretreatment includes mechanical processing (milling/grinding) and drying where the objective is to reduce the particle size but increase the surface area. Grinding of the dried feedstock into smaller particles on the order of millimeters and micrometers increases the surface area to mass ratio [49]. Simple drying in the relative absences of oxygen atmospheric conditions is the easiest pretreatment process to reduce the moisture of feedstock to below 10%wt. The drying approach can be divided into non-reactive drying reactive drying and torrefaction. Low temperature heat treatment leads to a shrinkage and reduced porosity of biomass, while heat treatment results in degradation and carbonization. The advantages of dry approach reduce biomass transportation cost, grinding energies, increases biomass stability and improve conversion to liquid product[50].

2.5. Biomass conversion processes

Biomass can be converting through a variety of thermochemical processes, as combustion, gasification, pyrolysis and liquefaction or through biochemical processes.

Biochemical processes use microorganisms or enzymes to break down the organic material into chemicals, including liquid and gaseous fuels as biogas, ethanol, methanol or biodiesel. The thermal processes are those in which dry biomass are subjected to high temperature and vary atmospheres of oxidation to release the chemical energy contained in biomass transform it into heat, mechanical energy or electricity or into different chemicals.

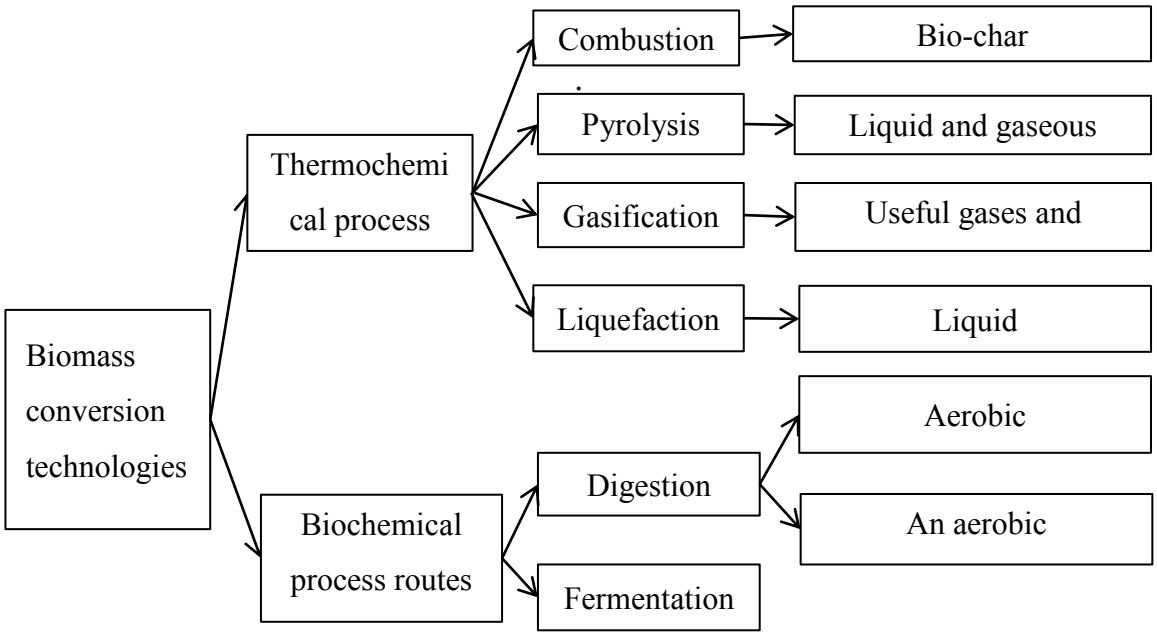

Figure 2.4: Various technologies used for biomass conversion [51], [52].

Pyrolysis is the process of thermal degradation when samples are heated at high temperatures and in an inert atmosphere (total absence of oxygen). After an initial stage of drying when the moisture is released, takes place an exothermic dehydration, when the inherent water and some low-molecular weight gases like CO and CO_2 are released. The next stage is the main devolatilization, when the degradation of long polymer chains of hemicellulose, cellulose and lignin occurs, producing into bio-char, condensable gases and non-condensable[53]. The last step would correspond to the carbonization of the volatiles and the degradation of carbonaceous solid to produce char and non-condensable gases[54], [55]. The thermal degradation of lignocellulosic biomasses are a complex process, where reactions occur simultaneously to produce gaseous products as CO, CO_2, alcohols,

aldehydes acids, furan-ring products, anhydrosugars and it produces a bio-char residue formed by fixed carbon and ash [56].

Depending on the type of pyrolysis is used, the intermediate species formed during degradation of cellulose, hemicellulose and lignin can be cooled resulting in dark liquid that contains many reactive species this process is not exothermic, the interest in pyrolysis is due to that liquid product, a liquid fuel known as bio-oil, which stores the chemical energy contained in the biomass and its heating valve is about a half of a conventional fuel oil [57]. The pyrolysis process is divided into three types depending on the operating conditions used for slow, fast and flash pyrolysis[58].

2.5.1. Slow pyrolysis

Slow pyrolysis has been utilized for thousands of the years, primarily for the production of charcoal. Slow pyrolysis is a conventional pyrolysis process; whereby the heating rate is kept slow (approximately 0.1-1℃/s). This slow heating rate leads to higher char yield than the liquid and gaseous products. In slow wood pyrolysis, biomass are heated to ∼500 ℃ [59]. The vapor residence time in the reactor, gas-phase products have sample opportunities to continue to react with other products to form char [60].

2.5.2. Fast pyrolysis

This type of pyrolysis processes are lignocellulose processed by rapid heating of biomass to moderate temperature in the absences of oxygen and immediate quenching of the emerging pyrolysis vapour. Fast pyrolysis uses much fast heating rates (about 10-200℃/s), and is considered as a better process than slow pyrolysis for producing liquid or gases.
In fast pyrolysis the liquid product yield is higher since the fast heating rates allow the conversion of thermally unstable biomass compounds to a liquid product before they form undesired coke [61]. Fast pyrolysis technology can have relatively high energy efficiency and low investment costs compared to other processes.

2.5.3. Flash pyrolysis

Flash pyrolysis is an improved version of fast pyrolysis, whereby the heating rates are very high > 1000℃/s, with reaction times of few to several seconds. Due to the rapid heating rates and short reaction times for better yields this process requires smaller particles size compared to the other processes [62]. However, this process has some technological limitation, for instances; poor thermally stability and corrosiveness of the oil, increase of

the viscosity over time by the catalytic action of char; alkali concentrated in the char dissolves in the oil and the production of pyrolytic water [63].

Table2.4:- Main operating parameters for pyrolysis process [60].

Operating parameters	Slow pyrolysis	Fast pyrolysis	Flash pyrolysis
Pyrolysis temperature (°C)	300-500	500-700	700-1000
Heating Rate(°C/sec)	0.1-1	10-200	>1000
Particle size (mm)	5-50	<1	<0.2
Solid residence time (s)	300-550	0.5-10	<0.5

2.6. Mechanism of pyrolysis process

The biomass pyrolysis can be divided into two categories, such as primary and secondary mechanism. In the primary mechanism, volatile compounds are released, while the chemical bonds within the polymers are broken during biomass heating process [64], [65]. Furthermore, rearrangement reactions within the matrix of the residues take place. Some of the volatile compounds which are unstable further undergo additional reactions, which are defined a secondary mechanism [66].

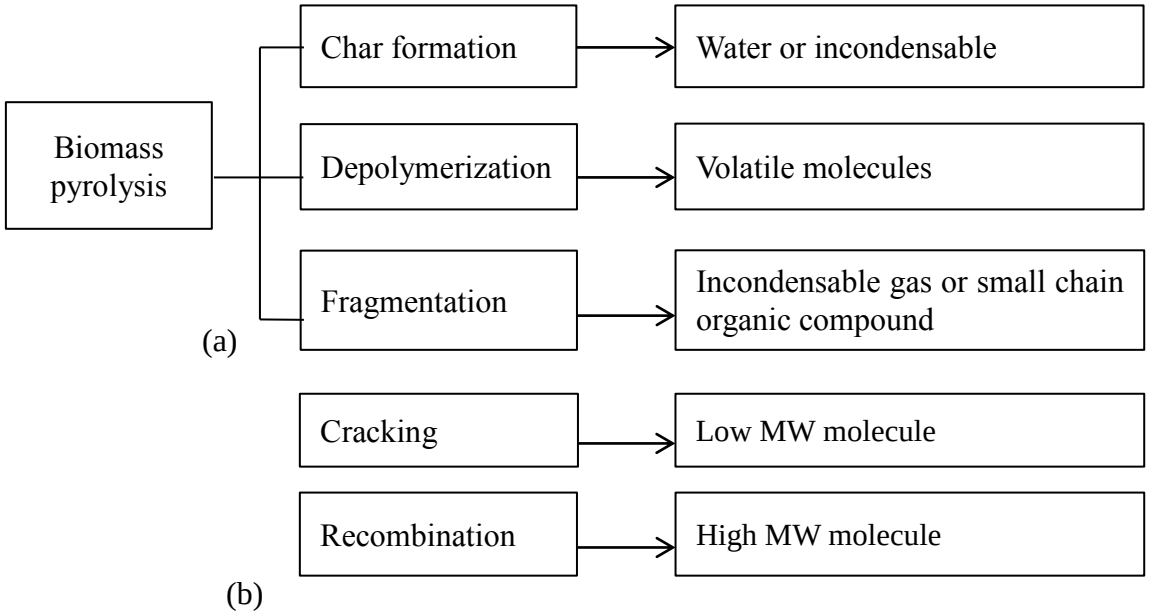

Figure 2.6:- Mechanisms of pyrolysis process (a) primary and (b) secondary mechanism.

The primary mechanism is explained in different three approaches, namely; char formation, depolymerization, and fragmentation. In the char formation process, initially, benzene rings are formed, and these rings combine into solid residue known as char, which is an aromatic polycyclic structure [67]. During this process, incondensable gas or water is

also released [68], [69]. In depolymerization process, polymers are broken into monomer unit which reduce the degree of polymerization. This process continues, until the volatile molecules are produced [70]. Finally, in fragmentation, incondensable gas and small chain organic compounds are formed through the linkage of many covalent bonds of the polymer, even within the monomer units [65].

The secondary mechanism consists of cracking, recombination and others [66], [71]. During cracking reactions, chemical bonds within the volatile components are broken, resulting in lower molecular weight products being formed [64], [72]. As the same chemical bonds can be broken within the polymer, there are similarities between fragmentation and cracking recombination consist[73]. Recombination consists of the association of two volatiles compounds to produces a new compound with higher molecular weight, which can be in volatiles at the reactor temperature. Secondary char can be formed when recombination reactions occur within the polymer matrix. The surfaces of the reactor, char or of an added catalyst can be also catalyzes secondary mechanism, resulting in the formation of secondary char at the surface of the catalyst material [71], [74].

2.7. Thermal decomposition of kinetics modeling

In the first attempt to understand biomass thermal behaviour and kinetics, were considered the classical mathematical methods developed in the 1960's. The assumed that the thermal decomposition of biomass could be well described by a single step reaction[20], [75], [76].Firstly the TG data need to be converted to normalized mass (W) using equation (2.1), where m and m_0 are the mass at a time t, and the initial mass, respectively.

$$w = \frac{m}{m_0} \quad \text{.....(2.1)}$$

The DTG curves determined by numerical differentiation have to be also normalized ($\frac{dw}{dt}$) using equation (2.2).

$$\frac{dw}{dt} = \frac{dm}{dt}\frac{1}{m_0} \quad \text{.....(2.2)}$$

For the kinetics analysis, it is necessary to select the main volatile release range from the normalized mass data. Then, using Eq (2.3) were converted in conversion, α, in which w_o, w and (w_f), the normalized mass at the beginning, at a time t, and at the end of the main volatile release, respectively.

The conversion (α) is a dimensionless measurement of the amount of reactants that has been converted into products. The experimental conversion rate ($d\alpha/dt$) is given by equation (2.4).

$$W = \left(\frac{w_o - w}{w - w_f} \right) \quad \text{.....(2.3).}$$

$$\alpha = \frac{dw}{dt}\left(\frac{1}{w_o - w_f} \right) \quad \text{.....(2.4).}$$

Generally the kinetic expressions for biomass a thermal decomposition can be express under isothermal or non-isothermal condition and formulated with respect to a combination of solid state reaction kinetic and Arrhenius equations.

For isothermal conditions, the form is

$$\frac{d\alpha}{dt} = k(T) f(\alpha) \quad \text{.....(2.5).}$$

$$k(T) = A\exp\left(-\frac{E}{RT} \right) \quad \text{.....(2.6).}$$

$$\frac{d\alpha}{dt} = A\exp\left(-\frac{E}{RT} \right) f(\alpha) \quad \text{.....(2.7).}$$

Where f(α) is the model, and it depends on the reaction mechanism, rate constant (k(T)), frequency (A), activation energy(E), absolute temperature (T), time(t), degree of conversion (α), and universal gas constant (R).

For non-isothermal form with accompanying heating rate, $\beta = dT/dt$ written as

$$\frac{d\alpha}{dT} = \frac{A}{\beta}\exp\left(-\frac{E}{RT} \right) f(\alpha) \quad \text{.....(2.8).}$$

Rearrangement and the integration of equation (2.8)

$$\frac{d\alpha}{f(\alpha)} = \frac{A}{\beta}\exp\left(-\frac{E}{RT} \right) dT \quad \text{.....(2.9).}$$

$$\int_0^{\alpha} \frac{d\alpha}{f(\alpha)} = A\exp\left(-\frac{E}{RT} \right)\frac{dT}{\beta} \quad \text{.....(2.10).}$$

In solid-state kinetics the Arrhenius parameters a rise form analogy with the representation of homogeneous kinetics (gas phase processes) by the collision theory of reaction rates.

From this statement, the activation energy (E) is the energetic barrier to be overcome in order to start a chemical reaction, i.e., reactants be converted in the products. The pre-exponential factor is the frequency of molecular collision during the reaction. Mathematical analysis to determine activation energy, frequency and reaction model was performed by the method of

- Model-fitting approach (Coats and Redfern).
- Model-fitting isoconversional (Kissinger-Akahira-Sunose and Ozawa-Flynn-Wall methods.

2.7.1. Model-fitting methods

Computational fitting methods are one of the most widely used methods in research. These methods assume a reaction model function f (α) and adjust the function with the experimental through non-linear least square fitting to obtain the kinetics parameters [57]. The simulation of biomass pyrolysis as just one component reaction is not accurate enough as already mentioned above. Thermal degradation of biomass is assumed to be the sum of the decomposition of its biomass component (cellulose, hemicellulose and lignin) [37]. The kinetics committees of the international confederation for thermal analysis and calorimetry published recommendation with the aim of improve kinetic analysis based on the experimental curves obtain by thermogravimetry techniques and differential thermal analysis. Among the recommendations mentioned it is included the comparison of the experiments at four different heating rates the quality of fit should obtain a correlation coefficient greater than 0.9 in the plot that compare the model with the experimental results, the use of an isoconversional method to verify the reliability of the calculated kinetic parameters and the validation of the rate expression with experimental data that have not been used to obtain the model [12].

2.7.2. Model- free methods

Model-free methods originated from the isoconversional principal which is often called the basic assumption. This assumption provides model free methods-the freedom to avoid the usage of theoretical kinetic methods for solid states kinetics with expression for f (α) and g(α) functions. The isoconversional methods are one of the most accurate kinetic methods to calculate parameters from thermochemical analysis[9].

The method is based on isoconversional principal that assumes that the reaction is a function that depends only in the temperature and its best property is that at it is not necessary to assume a previous reaction model to calculate the kinetic parameters [77].

The differential form is expressed by the Friedman method, whose expression is shown in equation (2.11)

$$\left(\frac{dT}{dt}\right) = \ln\left(A * f(\alpha)\right) - \frac{E}{RT} \quad \text{.....(2.11).}$$

The problem of differential method is thermogravimetric analysis result in a large amount of data which produce high level of noise when differentiate. To avoid this problem the integral methods was proposed. The form of the equation is expressed in equation (2.12).

$$g(\alpha) = \int_0^{\alpha} \frac{A}{f(\alpha)} d\alpha = \int_0^{\alpha} \exp\left(\frac{E}{RT}\right) dT \quad \text{.....(2.12).}$$

The most use integral method is the one developed by [78](OFW), who elaborates the following linear correlation to determine the kinetics parameter of biomass pyrolysis as a homogenous single reaction.

$$\ln(\beta) = -1.0518\left(\frac{E_{\alpha}}{RT}\right) + \ln\left(\frac{E_{\alpha}}{Rg(\alpha)}\right) - 5331 \quad \text{.....(2.13).}$$

Where β is the heating rate and g (α) is a conversion function. By linearizing the equation, the kinetics parameters are obtained with the slope of the curve.

The integral method is Kissinger- Akahira- Sunose (KAS) proposed in order to obtain more precision than FWO method in the numerical integration, calculating the apparent activation energy by linear regression analysis[79].

The KAS method is expressed equation (2.14)

$$\ln\left(\frac{\beta}{T^2}\right) = \ln\left(\frac{AR}{T}\right) + \ln\left(\frac{1}{g(\alpha)}\right) - \left(\frac{E}{RT}\right) \quad \text{.....(2.14).}$$

The problem to an integral method is to average the apparent activation energy which would cause errors in the calculation of the kinetic parameter during the numerical solution [80].

2.8. Catalytic cracking of biomass

Catalytic cracking is more appealing than thermal degradation on its own as it is faster and requires lower temperatures which significantly reduce the energy demand. Moreover, catalytic cracking using catalysts results in high quality products, therefore reducing the need for any further upgrade[21]. The pyrolysis of biomass involves the thermal decomposition in the absence of oxygen. During pyrolysis, the biomass materials are heated to high temperatures and thus, their macromolecules are broken into smaller molecules, resulting in the formation of wide range hydrocarbons. Using catalysts lowers the required pyrolysis temperature, reduces time of reaction and enhances the selectivity to specific component. However, catalyst regeneration is required due to coke formation[81].

2.8.1. Catalyst and support materials

A catalyst is defined as a material that accelerates a chemical reaction but remains unchanged chemically in the processes. For a reaction to be possible, the process must be accompanied by a decrease of activation energy. The reduction in activation energy is achieved by the catalyst providing an alternative pathway of lower energy for the reaction. Often products are formed in addition to those that are desired. The selectively of a catalyst is a measure of the catalyst's ability to direct the conversion to the desired products. The greater the stability of a catalyst, the lower the rate at which the catalyst loses its activity or selectively. Generally, catalysts consist of two or more components: the support and one or more active phases. The phase is principally responsible for the catalytic activity, while the support provides a vehicle for the active phase [82].

The activity of a catalyst has been related to the number of active (acid) sites on the catalyst surface [83]. Strong acids come in two fundamental types, Brønsted and Lewis acids. Brønsted acidity is provided by the very active hydrogen ion (H^+), which has a high positive charge density and seeks out negative charge, such as pi-electron in aromatic centres. Brønsted acids can add to an olefinic double bond to form a carbocation[84]. Catalyst used in the petrochemical industry includes amorphous, silica-alumina (SiO_2/Al_2O_3), zeolites and aluminium chloride ($AlCl_3$),amongst other[85], [86].

Now days, catalyst support are extensively used to decrease the costs and increase the constant surface area in chemical reactions. Specific surface area, compressive strength, pore volume and pore size are some of the most important characteristics of catalyst supports.

2.8.2. Catalyst and catalyst support selection

Different types of catalysts can promote different pyrolysis mechanism, resulting in different effects of pyrolysis temperature, product yields and qualities. Catalysts are selective towards specific bonds and different compounds therefore, the type of catalyst affects the temperature, bio-oil yield and composition [87]. Lignocellulosic biomass has been pyrolyzed using different composition of catalysts in the thermogravimetry. A review of these catalysts is given in this section. The bio-oil deoxygenation capabilities of the catalysts through decarboxylation, decarboxylation, and dehydration and associated with an increase in the HHV of the bio-oil.

The improvement of bio-oil quality will come at the expense of yield of organic fraction due to formation of CO_2, CO and H_2O in the deoxygenation process [88].

Numerous rereseach works has been carried out in the analyzing the effect of different cracking catalyst such as micro and meso-porous acidic zeolites, and metal oxides catalysts have been investaged in the literature.

2.8.2.1. Micro-and Meso-porous acidic

Zeolites are microporous and solid-acid aluminosilicate catalysts which have been studied extensively to upgrade bio-oil because of their similar use in the petroleum cracking industry. Zeolite catalysts have been shown to be effective in the deoxygenation of bio-oil, resulting in the formation of aromatic and effectively increasing the carbon-oxygen ratio in upgrading bio-oil. Zeolite catalyst (HZSM-5, β-zeolite, Y-type zeolite, ferrierite zeolite, MCM-41 and SBA-15) have use the bio-oil catalytic cracking [89]. Among these catalysts, HZSM-5 is most effective due to its high activity, strong acidity and shape selectivity [90]. Additionally, coke formation was a problem up to 16% of the original bio-oil ended up as coke deposits on the catalyst surface. However, HZSM-5 is easily deactivated by coking, resulting in low yields and short life cycle times. Small pores zeolites results in the increase of water and gaseous products, therefore reducing organic yield. Another disadvantage of zeolite structures is that they undergo irreversible deactivation when are dealuminated form the water produced by pyrolysis and catalytic dehydration [91]. The alkali and alkaline earth metals found in biomass irreversibly deactivated the HZSM-5 catalyst by substituting the proton of the acid site. This makes zeolite not appropriate for the in situ catalyst configuration where in the biomass is in contact with the catalyst [92].

2.8.2.2. Metal oxides

Metal oxides are known to improve bio-oil quality by deoxygenating and increasing heating value. Catalytic pyrolysis using Al_2O_3, CaO and MgO in particular, has been studied because they have been reported to 'be relatively inexpensive. Metal oxides, particularly transition metal oxides have been widely used as heterogeneous catalyst in various reactions. Generally, metal oxides possess either redox properties due to their multivant nature or certain acid-base properties which could potentially catalyze the thermal decomposition of lignocellulose and the reaction of pyrolysis intermediates to form more stable products.

i. Acidic metal oxide

Acid metal oxides, such as Al_2O_3, SiO_2 and TiO_2, have shown to decrease liquid yield while increasing gas and solid yield. Change in composition of bio-oil has been observed because of more production of aromatics and polyaromatic hydrocarbon, while actively removing oxygenated compounds (acids, ketones, aldehydes and inhibiting coke formation) [93].

For Acidic metal oxides such as Al_2O_3, SiO_2 and SiO_2- Al_2O_3 as well as the sulphated metal oxides such as SiO_4^{2-}/ TiO_2, SiO_4^{2-}/ ZrO_2, and SiO_4^{2-}/ SnO_2 have been investigated as catalysts in catalytically fast pyrolysis. The presence of acidic metal oxide also changes the composition of bio-oil. For Al_2O_3-catalyazed pyrolysis, there were many aromatic hydrogen and polycyclic aromatic hydrogen (PAH) in the organic products. SiO_2 with weak acidity and medium porosity was removing oxygenated compounds such as acid, ketones, and aldehydes and inhibiting coke and polycyclic aromatic compound formation in CFP of residue. Acidic metal oxides also catalyze the decarbonylation reaction and lead to increase of CO meanwhile the yield to C1-C4 hydrocarbon is also greatly increased [94].

Pyrolysis experiments with catalysts were carried out at a constant heating rate of 50^oC/min at the same temperatures use in non-catalytic runs to determine both effects of catalysts (ZnO and Al_2O_3) and catalyst ratio (5, 10, 15%) on the product yields. The liquid product yield, which was 41.89% without catalyst reached the maximum valve of 40.11% with 15% aluminium oxide catalyst at 350^oC.

In situ catalyst screening experiments with beech wood in a fixed bed reactor at 500^oC using various metal oxides (MgO, Al_2O_3, NiO, TiO_2 and ZrO_2) and a traditional zeolite

catalyst (ZSM-5) at C/B ratio of ½. MgO and alumina resulted in the most significant deoxygenation. The oxygen content of the bio-oil decreased from 41.68 wt. % to 21.94 and 24 wt. % with MgO and Al_2O_3 respectively, while the organics yield decreased from 37.37 wt. % to 15.02 and 16.62 wt. %. The pyrolytic water yield increased from 21.38 to 29.22 and 29.08 wt. % for MgO and Al_2O_3 respectively showing that dehydration reactions are responsible for improved deoxygenation [94].

Aluminium oxide means amphoteric oxide which is commonly referred as alumina. Porous gamma alumina is widely used as a catalyst support in chemical reaction such as a biodiesel synthesis via transesterification reaction and pyrolysis reaction. The superior properties of alumina support such as extreme thermal and mechanical stability, high specific surface area (as high as $300m^2/g$), meso-pore size (5-15nm), high pore volume ($0.6\ cm^3/g$), and its ability to be extrude and pelletized which make it a good catalyst support of active species with high catalytic in industrial process [95].

The common method used to produce supported catalyst (alkali metal and alkaline-earth metal affix on alumina support) is wet impregnation method. In such method, a suspension of the alumina powder support is treated with aqueous solution of active metal salt, and the resulting material is then thermal activated to convert the precursor to a more active state. Alumina is widely used as acid material of catalytic support because of its high chemical inertness particle size, which results in high activity of the surface of catalyst support [96], [97].

ii. Basic metal oxide

Base oxides are known to be active catalysts for ketonization and aldol condensation of carboxylic acid and carbonyl compounds. Alkaline earth metal oxides such as MgO and CaO are classic base. The addition of MgO decreased the yield to bio-oil but improved the bio-oil quality in terms of heating valve, hydrogen distribution, and removal of oxygenated groups. CaO catalyst is more cost effective, low toxicity, easy in preparation, and highly available.

Lu et al. found nano- CaO reduces the selectivity to phenols and anhydrosugars from 26.5% and 10.15% to 1.2 %, respectively, in non-catalytic fast pyrolysis. CaO eliminated the acids and increased the ketone selectivity from 3.8% to 20.9%, particularly the selectivity to cyclopentanones, which increased to 16.7% from 2.4% [89].

Catalytic pyrolysis process can be done with inexpensive base metal such as CaO, MgO, ZnO and dolomite, which reduce undesirable components from bio-oil. The use of CaO

and CaO. MgO (dolomite) reduce acidity and oxygen content. Accelerating aging test of bio-oil produced using CaO, MgO and ZSM-5 catalysts in fluidized bed reactor showed that CaO used bio-oil was more stable compared to other bio-oils.

In experiment using CaO catalysts for catalytic pyrolysis of corn cob showed that it helped to effectively reduce acids while improving the production of hydrocarbons. Even after the catalytic pyrolysis, oxygen content in the bio-oil is still high and makes it incompatible to petroleum fuels [98].

Metal oxides also exhibited good catalytic activity in bio-oil upgrading. For instance, nano MgO, CaO, TiO_2, Fe_2O_3, NiO, and ZnO were used in catalytic cracking of poplar wood pyrolysis vapors in a pyrolysis tube. The results indicated that CaO was the most effective catalyst increasing the formation of hydrocarbons, reducing the production of anhydrosugars, phenols and acids [89].

The CaO catalyst could increase catalytic decarboxylation by conversion of acid compounds to hydrocarbon. The acids can be eliminated and the levels of anhydrosugars and phenols can be reduced significantly. The formation of several light compounds, hydrocarbon and also cyclopentanones can also increase with CaO [99].

Catalytic pyrolysis of various biomass species with CaO, kaolin, and Al_2O_3 was investigated leading to production of a bio-oil with high PH, viscosity, and heating value. Regardless of the biomass type, CaO was found to produce bio-oil of lower viscosity than that of non-catalytic bio-oil compared to other catalysts used for their studies [100].

CaO has been reported to promote deoxygenation of bio-oils and increase its heating value and bio-oil oxygen content decreased from 39 to 31 wt. % with the use of CaO catalyst while, CaO was used as a catalyst, an increase in pyrolytic water yield or an increase in the bio-oil water content was reported while the total organics yield decreased [101].

Studied the effect of three different catalysts (CaO, MgO and ZSM-5) as bed materials and concluded that bio-oil from CaO catalytic pyrolysis was comparatively stable and had lowest TAN. They found ZSM-5 had very less effect on acid property even through it produced less acidic oil [102]. Alkaline earth metals are found in form of minerals and can be applied directly for catalysis without chemical treatment. The advantages of these materials are that they are abundant and are inexpensive compared to synthetic catalysts. The uncalcined forms of these materials are called limestone ($CaCO_3$), magnesium carbonate ($MgCO_3$), and dolomite ($CaCO_3$. $MgCO_3$). These materials show high catalytic

activities for tar elimination when calcined. Calcination is a process where bound carbon dioxide is released upon heating. Calcined forms include calcites, magnesites and dolomites [103].

2.9. Factor affecting pyrolysis process

The generation and distribution of the products will be conditioned by the physicochemical characteristics of biomass, despite the operating conditions being the same, due to its effects on heat and mass transfer along the particle. The influential factors in pyrolysis process are particle size, heating rate and catalyst loading.

2.9.1. Particle size

One of the most influential in factors in pyrolysis and combustion processes is particle size. A bigger particle size increases the resistance for the condensable gases to leave the particle, which favours the occurrences of secondary reactions between the volatiles phases coming from the interior of the particle with the carbonized material that has already reacted on the surface of the particle [104], [105].

Reversely, a finer particle size enables the movement of the primary products through the particle, which increase the liquid yields[51]. Primary pyrolysis releases CO_2, while secondary pyrolysis produces mainly CO and CH_4. Because of the fact that particle size is a parameter that has been given great importance in the literature, many researches have been carried with the aim of determining the effect of particle size on the thermal behaviour of biomass. Some of these studies often differentiate particle by size groups as for example [54], who separated the particles into three categories:-

- Small particles(112-125μm)
- Medium particles(500-600μm)
- Large particles (800-1000 μm)

It can be concluded that the thermal behaviour of the particles large and medium particles is the same, whereas the behaviour of the small particles deviates in the final stage of conversion curves and predicts as faster devolatilization. The explanation proposed was that the kinetics of larger/ medium particles incorporates the effects of internal heat transfer resistance, which means that kinetics can predict the thermal behaviour of particles, either medium or large, and that the effect of particles size can be considered negligible.

2.9.2. Effect of heating rate

Most of the TGA experiments have been performed under low heating rate conditions (less than 50^{o}C/min) because high heating rate TGA measurements are rather complex. However, heating rates of TGA experiments influence the characteristics of thermogravimetric curves. Indeed, the pyrolysis rate is affected by the heating rate in the particle and it leads to different kinetics parameters. Therefore, it is to known under which conditions pyrolysis occurs in low/high heating rate regimes in order to apply the appropriate TGA kinetic parameters[104]. The rate of heating is one of the important factors in the process of pyrolysis and the combustion of biomass[106].

- High heating rates contributes to formation of volatiles and consequently to the production of liquid. Higher heating rates also favours the formation of temperature gradients inside the particle, which as mentioned above, promotes the appearance of secondary reactions, which results in a secondary char formation.
- Lower heating rates produce more char as it provides more contact time between the volatile phase and the solid phase.

2.9.3. Catalyst loading

Pyrolysis product yield are party dependent on the catalyst to biomass ratio. Using catalysts at very high catalyst to biomass ratios of greater than 1/1i.e. more than 50 wt. % catalyst, poor bio-oil yields were observed as well as increases in the gas and char yields[107]–[109]. However, the bio-oil quality in terms of deoxygenation and energy content increased. The presence of large amounts of catalyst in the feedstock is believed to enhance the cracking of vapour resulting in an increased incondensable gas fraction [110]. Also, some secondary reactions of the volatiles leading to the formation of high molecular weight compounds (recombination) are promoted. These compounds generate carbonaceous deposits and hence increase the char yield. It was observed that changing the catalyst to biomass ratio of 1/3 to 3/1 resulted in an increase in the char yield from 27 wt. % to 44 wt. % on a catalyst free basis [107]. A lower catalyst concentration means that the available active catalyst surface area is limited, thereby allowing some of the volatiles to exit the reactor unreformed and leading to limited deoxygenation. Therefore, the catalyst to biomass ratio must be optimized in the range 0/1-1/2 i.e. 0-50 wt. % catalyst for an efficient and economic catalytically pyrolysis process.

CHAPTER THREE

3. METHODOLOGY

The experimental work was done in the laboratory of Adama Science and Technology University, School of Mechanical, Chemical and Material Engineering and Bahir Dar University, School of Biochemical and Chemical Engineering.

3.1. Materials and equipment

Corn cob that used for catalytically thermal degradation pyrolysis experiment in this study.

All chemicals used in this study were aluminium nitrate non-a hydrates (Al $(NO_3)_3.9H_2O$), urea, calcium carbonate and distilled water. The major equipment's used in this study were Digital balances, spatula, Measuring Cylinder, Conical flask, beaker, petri dish, crucible, magnetic stirrer, ball mill, sieves, oven, box-type resistance furnace, dissector, SEMEDX analyser, bomb calorimeter, thermogravimetry (Beijing, HCT-1), X-ray powder diffraction (XRD-7000), Scanning electron microscopy, Fourier transforms infrared spectrum (FT/IR-6600), Tong, glove and face mask were used for safety.

3.2. Method

3.2.1. Preparation of corn cob

The corn cob sample was collected from agricultural field locally (Finote Selam Amhara Region, Ethiopia). The samples were dried in the sun for a few days to remove the moisture content so as to a void the growth of fungus and gred mould. The corn cob were dried again in the conventional oven at 103±0.5^{o}C, until their moisture content achieved less than 10 wt. % of moisture content and it was into powder in a laboratory a high-speed rotary ball mill and sieved with a100-mesh sieve (< 250μm) [111]. The material that passed through the sieve were gathered in two different closed containers and kept for analysis.

3.2.2. Characterization of corn cob

The proximate analysis was conducted on a received basis, while ultimate analysis and heating value was performed on a dry basis.

3.2.2.1. Proximate analysis

Proximate analysis is used for calculation of chemical composition of the residues, including moisture content, ash content, volatile mater and fixed carbon.

i. Moisture content

Moisture content is calculated by measuring a known quantity of air dried corn cob ASTM D-871-82. Finely corn cob was taken on petridish and kept at a temperature of 103^{o}C for 16 hour. Before and after heating weight of sample were measured and recorded. The difference in weight divided by initial sample weight gives moisture content[111]. Maximum the moisture content, high is the transportation cost and lower is the caloric valve. Thus, low moisture content in biomass is preferable.

$$\%MCC = \frac{M_{initial} - M_{dried}}{M_{initial}} \quad \text{.....(3.1).}$$

Where: %MCC (percentage of moisture content), $M_{initial}$ (before dry base of corn cob) and M_{dried} (weight of corn cob material).

ii. Volatile matter

When fuel is heated, volatile matter of a fuel are released in form of condensable and non-condensable vapour. The amount of released vapors i.e. volatiles matter depends on the rate of heating and the temperature to which it is heated. The applicable ASTM standard for determination of volatile matter is ASTM D-3157-07. 1g powered sample after removing moisture was taken in a crucible covered with lid and kept at 950^{o}C for seven minute [112]. Volatile matter can expressed in terms of mathematically determined by following expression

$$\%VM = \frac{w_{to} - w_{tx}}{w_{tx}} \quad \text{.....(3.2).}$$

Where: %VM (percentages of volatiles), w_{to} (weight of initial mass of cut-off sample) and w_{α} (weight of cut-off sample at a particular temperature).

iii. Ash content

The final residue left after the complete combustion of sample is ash. It was found out by heating 1g of sample at 575±25^{o}C for three hour without lid. Ash, the inorganic solid residue left after fuel is completely burned, has primary ingredients such as silica,

aluminium, iron and calcium and sometimes small amounts of magnesium, titanium, sodium, and potassium. Ash content is determined by ASTM D-1102 [113].

$$\%ACC = \frac{W_{ash}}{W_{cc}} * 100 \quad \text{.....(3.3).}$$

Where: %ACC (percentage ash content of corn cob) W_{ash} (weight of ash content) and W_{cc} (weight of corn cob)

iv. Fixed carbon

Fixed carbon may also be determined using empirical formulae, by subtracting the sum of the experimentally determined moisture, ash and volatile matter experimental contents from 100 (% mass) [114], as in Equation

$$\%FC = 100 - (\%MCCdb + \%ACC + VMdb \quad \text{.....(3.4).}$$

3.2.2.2. Ultimate analysis

This analysis is important for determining the elemental composition (C, N, H, S, and O) of the biomass fuel and is also useful for calculating their calorific valve. It can be carried out by using SEMEDX analyzer.

3.2.2.3. Heating valve

The corn cob was obtained from available sources. They were separately dried crush-grinded and sieved through a 250 micrometer sieve to remove the granular impurities and the samples powders, which tend to influence the result. The corn cob is then pressed using the laboratory scale tablet machine which binds the powdered samples into convenient form for use in the bomb calorimeter that cannot be easily disintegrated. 1-1.3 g each of the prepared sample of corn cob were collected and transferred to the sample cup of the bomb calorimeter making sure the interior of bomb including the support and crucible are properly cleaned and dried. A 10cm long Nichrome wire was fixed to the two electrodes and the sample cup containing the sample was carefully fixed into the electrode seat inside the bomb. Pressed pellets were used to prevent splashing and incomplete combustion of the sample in the calorimeter [115].

The decomposition vessel, in which both the sample pellet and ignition wire were located, was filled with oxygen (99.995 %) at a pressure of 15-20bar to produce complete combustion. The recipient was also immersed in water so that the initial temperature of the

sample was 22 ◦C. When complete combustion occurs, the biomass sample releases an amount of heat that is measured as the temperature difference in the calorimeter. The device was calibrated with benzoic acid pellet [116]. Corn cob samples were analyzed in triplicate to guarantee reproducibility of the method.

The standard deviations were also calculated for these experimentally obtained values.

$$\varepsilon = \frac{m_{ba} * q_{vba} + Q_{fuse} + Q_{ign}}{\Delta T} \quad \text{.....(3.5).}$$

Where, m_{ba} = mass of benzoic acid (g), q_{vba} = gross calorific value of benzoic acid (J/g),

Q_{fuse} = heat attributed to the cotton thread (J), Q_{ign} = heat attributed to the Nichrome ignition wire (J) and ΔT = corrected temperature rise of the calorimeter vessel (K).

With the knowledge of the calorific values of the leftover fuse wire and cotton tread, the corrections can be made to test corn cob sample calorific valve using the following formula:

$$q_{vcc} = \frac{\varepsilon * \Delta T - Q_{fuse} + Q_{ign}}{m_{CC}} \quad \text{.....(3.6).}$$

Where m_{cc} = mass of corn cob

3.2.3. Synthesis CaO/γ-Al_2O_3 catalyst

3.2.3.1. Preparation of γ-Al_2O_3

Aluminium nitrate nonahydrate (Al $(NO_3)_3.9H_2O$) dissolved near its saturation point (28 g/ 40ml H_2O) in deionized water at 22^oC under magnetic stirring. Then, it will follow by addition of urea (61g/60ml H_2O) and kept at 22^oC for 1hr on the hot plate and magnetic stirrer. Aluminium nitrate nonahydrate-urea saturated solution is heated in the oven for 24hr at 90^oC. Heating the solution gave a sol at the first step and further heating of a sol finally end up yielding a transparent gel. This gel will be a white crystalline and lustrous solid. Alumina gel will then got dried at 280^oC for 1hr to eliminate urea and nitrate left unreacted inside the gel. This procedure result is a porous and amorphous gamma solid. A solid gamma alumina obtained will then milled finely to increase the surface area.

3.2.3.2. Synthesis of CaO/γ-Al_2O_3 catalyst

CaO/γ-Al_2O_3 catalyst was synthesized by employing the method of impregnation primarily, the measured weight of $CaCO_3$ (a precursor to CaO) (0 wt.%, 10 wt.%, 20 wt.%, 30 wt.%, 40 wt.%, and 50 wt.% CaO by weight of γ-Al_2O_3) dissolved in 50ml of deionized water under magnetic stirrer at room temperature. Then, the weighed mass of γ-Al_2O_3 powder was mixed with $CaCO_3$ solution and stirred over γ-alumina and let dried in the oven at 105^oC for 24h. Then, then dried mass was calcined at 700^oC for 4:30hr to liberate carbon dioxide, physically absorbed and chemically bonded moisture.

3.2.4. Characterization of CaO/γ-Al_2O_3 catalyst

3.2.4.1. Thermal stability of catalyst

Thermogravimetric analysis was performed using (Beijing, HCT-1, TGA) analyzer. The corn cob feedstock was loaded in a high purity alumina pan with approximately 8mg weight of the powdered sample. Nitrogen was used as carrier gas for creating the inert environment. The heating rate was set at 20^oC/min and the temperature range is between 20^oC to 800^oC. This analysis produced two types of curve, TG curve and derivative thermogravimetric (DTG) curve. TG curve represents the change in weight of the sample as a function of temperature. The DTG curve indicates the rate of weight change, dw/dt versus temperature [117].

3.2.4.2. Morphology study of CaO/γ-Al_2O_3 catalyst

Scanning Electron Microscopy (SEM) is resolution imaging system with an extraordinary depth of field. It indicates topographical, structural, and elemental data at low magnifications up to 200,000. The morphology, structure and elemental data of CaO/γ-Al_2O_3 were done by scanning electron microscopy (SEM).

3.2.4.3. Crystalline structure and phase of catalyst

Phase identification and crystalline structure of the CaO/γ-Al_2O_3 catalyst was done by X-Ray diffraction (XRD) is a rapid analytical technique primarily used for phase identification of a crystalline material and can provide information one unit dimensions. Monochromatic X-ray as a sources of radiation containing Cu-Kα (λ = 1.5405 Å) with 40Kv power and 35 Ma current was directed toward the sample. Each sample was scanned within the 2θ range of 10-80^o and intensity was measured. Crystallite size in the prepared

sample was calculated by using the data from the XRD pattern by using the Scherrer formula,

$$D = \frac{\kappa\lambda}{\beta \cos\theta} \quad \text{.....(3.7).}$$

Where,

D = crystallite size

λ = wavelength of the X-rays produced in the machine

β = width of a peak at half of its intensity

θ = angle of the corresponding peak

k = shape factor

3.2.4.4. FTIR analysis

Fourier transforms infrared (FTIR) spectra analysis of the $CaO/\gamma\text{-}Al_2O_3$ catalyst in the range of 4000-400cm^{-1} using Fourier transform infrared spectrophotometer. FT-IR spectroscopy study was operated with KBr disc method. Sample preparation involved mingling of 40mg fine powder of calcined or activated with 150 mg KBr powder, milling in gate mortar and compressing it to make a pellet. The catalyst sample study was then performed in the transmission FTIR spectroscopy.

3.2.5. Catalytically thermal degradation of corn cob

Thermogravimetric analysis involves monitoring the weight loss of the sample as controlled function of temperature. An important application of TG in the study of corn cob is the measurement of thermal stability. In this study, the analysis serves primarily as an assessment tool of various potential catalysts for corn cob pyrolysis. An assessment of the catalyst performance prior to use in the reactor reduce costs. Furthermore, this particular TG model allows for the variation of parameters such as the heating rate. In addition, to the mass at each temperature change, the data output also includes time and rate of weight loss (DTG) at each temperature step [118]. The heating rate feature and time data are particularly important of the pyrolysis, which will be discussed in section 3.2.5.1.

3.2.5.1. Thermogravimetry sample preparation

In the Thermogravimetry study of catalytic degradation of corn cob by 10 wt.%, 20 wt.%, 30 wt.%, 40 wt.% and 50 wt.% $CaO/\gamma\text{-}Al_2O_3$ catalyst prepared their samples by mixing dried proportions of corn cob and catalysts (mechanical mixing). In this analysis, they found the amount of catalyst to be different for runs at the fixed process parameters such as particles size, temperature, heating rate, and catalyst loading in TGA equipment. This makes to assess the extract performance of the catalysts in the decomposition of curves.

3.2.6. Effect of catalyst loading and heating rate

3.2.6.1. Effect of catalyst loading

Thermogravimetric analyser was used to investigate the thermal degradation behaviour of catalytic pyrolysis of corn cob at different catalyst weight loading. There are four samples used as feedstock for TGA. These samples are added with different catalyst weight loading (2, 4, 6 and 8%). The prepared samples approximately 8-12mg were first heated to 105°C and kept at that temperature for about 30 min to remove any moisture content from the sample. After that the samples were individually heated to a maximum temperature of 800°C in an inert (N_2) atmosphere flowing at 50 mL/min at fixed heating rate of 20 °C/min [119].

3.2.6.2. Effect of heating rate

The pyrolysis experiments were performed at heating rates of 5, 10, 15 and 20ºC/min from ambient temperature to 800ºC. During heating, mass and temperature of the sample were simultaneously and continuously recorded. In the pyrolysis experiments, N_2 of ultra-high purity was passed through the TGA at a constant flow rate of 50 mL/min to provide the inert gas environment and to sweep away the volatiles released [120].

3.2.7. Determination of kinetics parameters

The kinetics parameters were determined by the Microsoft excel 2010 software package.
This program among other things facilities kinetics analysis of thermogravimetric analysis data for the study of catalytic degradation of corn cob. The method determines the kinetic parameters activation energy and pre-exponential factor of a given solid material and predicts reaction progress under arrange of temperature (up to 800ºC) and heating rates (5, 10, 15 and 20ºC/min). The kinetics parameters, activation energy and pre-exponential, reaction progress and thermal stability of corn cob under a temperature range of up to

800^{o}C were determined [121]. The following steps were used to estimate the non-isothermal catalytic parameters of corn cob.

3.2.7.1. Determination of activation energy

The activation energy can be solved by isoconversional (Flynn-Wall-Ozawa and Kissinger-Akahira-Sunose method) form equation (2.13) and (2.14).

3.2.7.2. Degradation mechanism

Model fitting method is a reaction model exploring method using well-known different theoretical reaction models to fit experimental α-T profiles, meanwhile for each model asset of activation energy and pre-exponential factor can be obtained. The Coats-Redfern method is one commonly used model fitting which explores the asymptotic series expansion with the following formula [122],

$$\ln\frac{g(\alpha)}{T^2} = \ln\left(\frac{AR}{\beta E_\alpha}\left(1-\frac{RT}{E_\alpha}\right)\right) - \frac{E_\alpha}{RT} \quad \text{.....(3.8).}$$

Where g (α) is the integral form of the reaction model as shown in table, and T_{averge} is the average temperature during all the heating process. For each reaction model as listed in Table 3.1: plotting ln [g (α)/T^2]vs.1/T can obtain sets of activation energy and pre-exponential factor.

Table 3.1: Fourteen different kinetic models and their integral g (α) and conversion [14].

Kinetic model	Symbol	g(α)	α
Chemical reaction			
Frist order	F1	$-\ln(1-\alpha)$	$1-\exp(-z)$
Second order	F2	$(1-\alpha)^{-1}-1$	$1-(1/(z+1))$
N^{th} order	Fn	$((1-\alpha)^{1-n}-1)/(1-n)$	
Diffusion			
1-D diffusion	D1	α^2	$z^{1/2}$
3-D diffusion	D3	$[1-(1-\alpha)^{1/3}]^2$	$1-[1-z^{1/2}]^3$
Phase-boundary reactions			
Contracting area	R2	$1-(1-\alpha)^{1/2}$	$1\ (1-z)^2$
Contracting volume	R3	$1-(1-\alpha)^{1/3}$	$1-(1-z)^3$
Power law			
	P4	$1/4\alpha$	z^4
	P3	$1/3\alpha$	z^3
	P2	$1/2\alpha$	Z^2
	P2/3	$3/2\alpha$	$z^{2/3}$
Nucleation and growth			
	A2	$[-\ln(1-\alpha)]^{1/2}$	$1-\exp(-z^2)$
	A3	$[-\ln(1-\alpha)]^{1/3}$	$1-\exp(-z^3)$
	A4	$[-\ln(1-\alpha)]^{1/4}$	$1-\exp(-z^3)$
	A3/2	$[-\ln(1-\alpha)]^{2/3}$	$1-\exp(-z^{3/2})$

Where $z = \frac{ART}{\beta E}(1-\frac{2RT}{E})\,e^{\frac{-E}{RT}}$

3.2.7.3. Invariant parameter techniques

Model-fitting methods involves the use of different reactions models to fit one single conversion curve or multiple curves, and then attempt to determine the kinetics parameters and by regression analyses. When a model-fitting method is applied to a single-heating test, widely varying values of the activation parameters are obtained when using different model functions E and A that can be correlated to the compensation effect relation.

$$\ln A = a + bE \quad \text{.....(3.9).}$$

Where, a and b are constants. It has been theoretically and experimentally postulated that reaction rate.

All model listed can be examined by Coat-Redfern method by which nineteen corresponding sets of kinetics parameters can be examined can be obtained. Then the calculated activation energy and per-exponential factor can be used to evaluate the compensation effect formula parameters a and b. based on the obtained compensation effects formula, the pre-exponential factor at each conversional extent can be evaluated according to activation energies obtained by isoconversional methods.

3.2.7.4. Kinetic mechanism screening

The model which has the best linearity with experimental profile is considered as the real reaction model. There are fourteen commonly used reaction models in a kinetics area. Each model will be used to fit the experimental formation with the obtainment of activation energy and pre-exponential factor. Then, according to the fitness of experimental data and theoretical model calculation, one correlation coefficient can be obtained. So, for all fourteen models, there must exist one maximum correlation coefficient.

CHAPTER FOUR

4. RESULT AND DISCUSSION

In this section the study discussed proximate, ultimate analysis and heating value of the sample, characterization of catalysts, effects of biomass to catalyst ratio and heating rate catalytic thermal degradation of corn cob and activation energy and pre-exponential factor were analyzing using thermogravimetric analysis.

4.1. Characterization of corn cob

4.1.1. Proximate analysis

The moisture, ash, volatile matter and fixed carbon content in the biomass were determined by proximate analysis. The fuel's quality and type can be determined quickly and easily by this analysis. Conversion efficiency and heating value of biomass drastically depend upon the moisture content. Biomass, during storage decomposes more rapidly if the moisture is lower. After pyrolysis, volatiles matter convert in the form of light hydrogen, gas and tars. Corn cob contains around 78% of volatiles matter, which is higher than the coal[123]. Due to higher content of volatiles matter, biomass devolatilize readily than solid fuel. Also, biomass liberates less fixed carbon, which is for pyrolysis. Along with moisture content, ash content also affects the heating value. As the plant structure include of a wide variety of mineral matter (potassium, calcium, magnesium, silica and ash content) are vital part of biomass. Ash content varies with plant and soil condition, weather conditions. From proximate analysis result of corn cob has higher percentage of volatile matter and less amount of ash content compared with other agricultural resides. The results of experimental analysis that the agricultural waste (corn cob) used in this work produced more heating value than the popular charcoal being used for cooking. The calorific values are in the order of Maize cob greater than Charcoal with the following values 18.23KJ/g and 10.21KJ/g respectively. These values met the minimum standard calorific value of 6.276 KJ/kg – 6.988cal/kg by Álvarez-Álvarez et al., 2018.

Table 4.1: Proximate analysis results of corn cob (as received basis).

Content	This study Weight (wt. %)	Demiral et al. (wt. %)	Liu et al. (wt. %)	Trninić et al. (wt. %)	
				Hawaiian CC	Serbian CC
Moisture	6.42±0.52	7.36	11.7	-	-
Ash	2.2±0.2	1.49	2.7	2.6	1.5
Volatile matter	78.0	79.56	69.5	79.6	81.1
Fixed carbon	15.345±0.526	11.57	15.9	17.5	17.5
Heating value (KJ/g)	18.23	-	13.4	-	-

4.1.1. Ultimate analysis

The ultimate analysis is the determination of elemental composition of biomass (carbon, hydrogen and oxygen). Obtained results that the carbon content higher than 50% and their composition owned lower amount of oxygen. The high proportion of carbon leads to increase of calorific valve. The corn cob composition of sulphur and nitrogen are very small amount moreover, indicated using corn cob in thermochemical conversion process have insignificant production of NO_x and SOx to pose any pollution threat. According to previous studies, the nitrogen and sulphur content are 0.43% and 0.2% for corn cob. As evaluated, the amount of nitrogen and sulphur were very low, so that they were all neglected in our studies[124]. As compared to literature data, corn cob used in this work can act as good solid fuel and useful towards the products (solid, bio-oil, and gases)[124]. Sulphur content may also cause the corrosion towards equipment (pyrolysis reactor) by sulphric acid formed during and after pyrolysis process. From here, the biomass used in this work can reduce the corrosion severity impact towards the equipment use and can reduce the cost for maintenances. In most cases, biomass considerably has less sulphur content than a coal. Meaning that, an increasing of biomass as thermal output makes the SO_2 emission decrease proportionality. From the literature data corn cob of biomass showed the value in the range of the standard agriculture wastes ultimate analysis which is C (40-53), H (4.5), O (31-52), N (0.0-0.7) and S (0.1-8) as stated[9]. The results of SEMEDX analysis in the composition of corn cob consists of 51.43% carbon (C) and 42.85% oxygen (O).

4.2. Characterization of CaO/γ-Al_2O_3 catalyst

4.2.1. Thermogravimetric analysis

Thermal analysis of synthesized γ-Al_2O_3, CaO, 10 wt. % and 50 wt. % CaO/γ-Al_2O_3 catalysts are shown in Figure 4.1 γ-Al_2O_3, catalyst started to decompose at around 40^oC and completely decomposed at 590^oC. The γ-Al_2O_3 TGA analysis suggests that some water could be desorbed at temperature from 30 to 220^oC[125]. The decomposition of 10 wt. % CaO/γ-Al_2O_3 up to 300 ^oC was lower than that of γ-Al_2O_3. This could be related to hygroscopic nature of the catalyst. The catalyst maintained its stability within (300 ^oC-700^oC). Two mass loss steps were observed with different change in mass. The loss of mass between 40 and 300^oC can be attributed primarily to moisture content of 10 wt. % CaO/γ-Al_2O_3, while the second decomposition occurred at 700-800^oC. The pure CaO and 50 wt. % CaO/γ-Al_2O_3 catalysts were thermally stable up to 722^oC as shown in Figure 4.1; there is no significant change or weight loss of sample. The TGA of CaO and 50 wt. % CaO/γ-Al_2O_3 show high thermal stability with only one stage degradation at elevated temperature 722^oC. Specifically, in case of the 10 wt.% CaO/γ-Al_2O_3 catalysts the TGA curves shows 14% weight loss in the temperature range 40-150^oC, due to desorption of physisorbed water molecules. A 5% weight loss in the region of 150-300^oC is attributed to the decomposition of the precursor and removal of chemisorbed water. From the obtained thermal properties; the synthesized CaO, 10 wt. % and 50 wt. % CaO/γ-Al_2O_3 catalysts can be used as a catalyst during thermal degradation of corn cob and other biomasses. Generally, thermal stability of the catalyst increased with an increase in CaO/ γ-Al_2O_3; CaO > 50 wt. % CaO/γ-Al_2O_3 > 10 wt. % CaO/γ-Al_2O_3 > γ-Al_2O_3. It has been proved that γ-Al_2O_3 was a good support since it has high surface area[126].

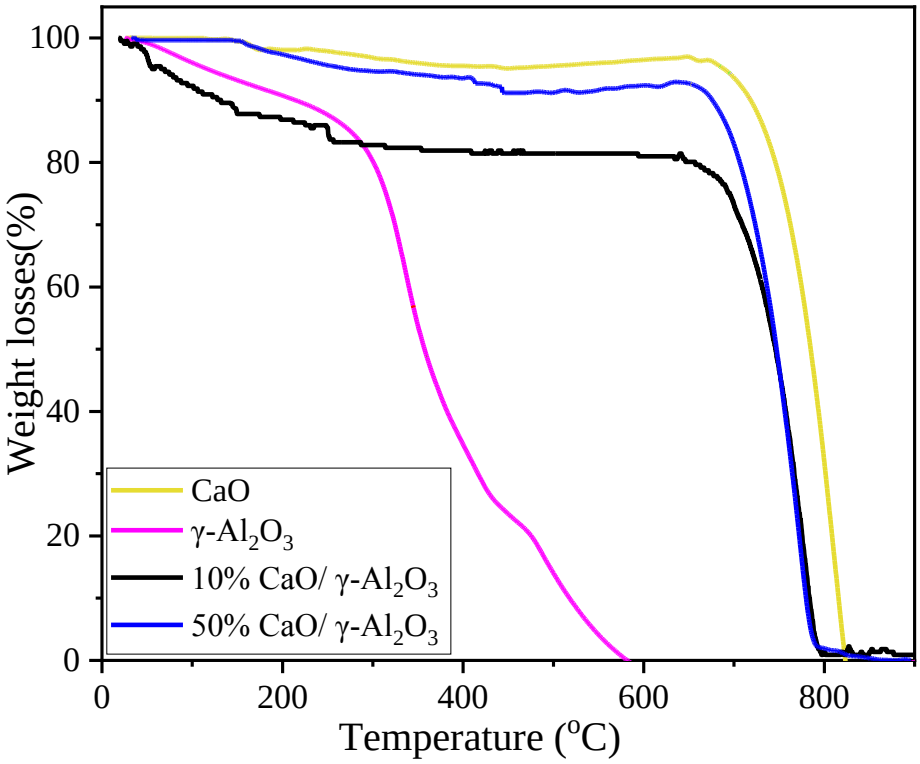

Figure 4.1: Thermal stability of catalyst.

4.2.2. Morphology study of CaO/γ-Al_2O_3 catalyst

The surface morphology of γ-Al_2O_3, 10 wt% and 30 wt% CaO/γ-Al_2O_3 catalysts were studied by SEM analysis. As illustrated in Figure 4.2a, the γ-Al_2O_3 has a very high non-uniform amorphous structure, which in a good agreement with samples high surface area and structure. Figure 4.2b-d, shows the surface morphology of calcium oxide-gamma alumna catalysts with various amount of calcium oxide loading into support (composition of calcium oxide increase with reducing the surface of the catalysts)SEMEDX result showed that the sample have a porous and homogeneous aggregates (10% cases). The EDX Result confirmed the presence of Al, O and remaining impurities N. The EDX graphs below also confirmed the presence of Al, O and well dispersed Ca. there is also some remaining C.

.

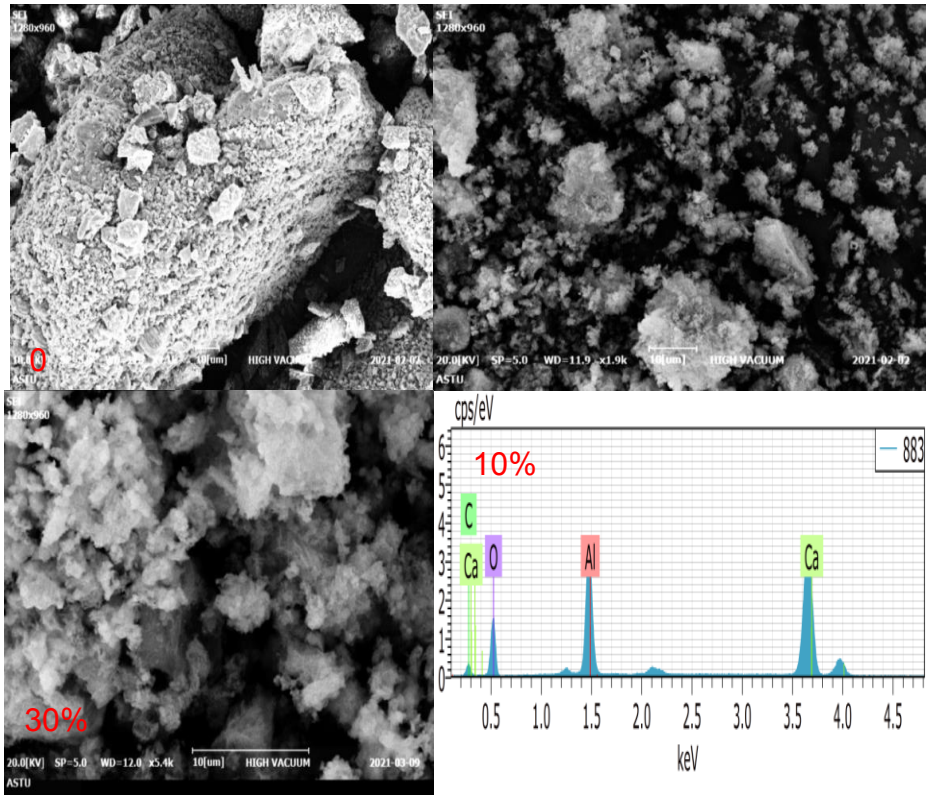

Figure 4.2: Surface morphology of (a) γ-Al_2O_3 (b) 10 wt. % CaO/γ-Al_2O_3 (c) 30 wt, % CaO/γ-Al_2O_3 and (d) 50 wt. % CaO/γ-Al_2O_3.

4.2.3. Crystalline structure and phase of catalyst

XRD analysis was performed to the study of the crystalline structure of samples. Figure 4.3: shows that XRD patterns of pure γ-Al_2O_3 and 50 wt. %, 30 wt. % and 10 wt. % CaO loaded on γ-Al_2O_3. The XRD pattern of gamma alumina shows the diffraction peaks at 11^o, 29.7^o, 33.8^o, 44.12^o and 64.4^o [127].The two peak appeared at around ($2\theta = 44.12^o$ and 64.4^o) are the common peaks of gamma alumina[96], [97]. The intensity of XRD peaks and the peak width indicate that large amount of amorphous γ-Al_2O_3 was formed. The peak observed at 11^o is probably due to the impurities associated with nitrates. It is also observed that this peak was totally eliminated at higher calcination temperature. The XRD patterns of the γ-Al_2O_3 samples loaded with 50 wt. %, 30 wt. %, and 10 wt. % CaO are presented in Figure 4.3; all samples were calcined at 700 for 4:30 hr. When the calcium oxide was loaded on γ-Al_2O_3 support, the diffraction peaks of γ-Al_2O_3 shifted to higher angle; this was due to diffusion peak of CaO particles into the support structure. Powder X-ray diffraction typical peaks found at $2\theta = 18.01^o$,23.4^o, 34.5^o, 37.5^o, 43.2^o, 47.5^o and 48.6^o) confirm the presence of CaO/$CaCO_3$ for all catalyst sample loaded with CaO[128].

Specially, the peak at $2\theta = 37.5^{o}$confirm the presence of CaO. Despite the fact that most of metal carbonate precursors were broken down to the corresponding metal oxides by releasing off carbon dioxide, a very small amount of metal carbonate has been left in the catalyst. In line with this, the peaks at $2\theta = 36.3^{o}$ and 39.57^{o} are probably due to the presence of $CaCO_3$ for the 50 wt% and 30 wt% CaO catalyst loaded on γ-Al_2O_3. However, this peak was not observed for 10 wt% catalyst loaded on γ-Al_2O_3. The sharp peak at $2\theta = 29.5^{o}$ could also be related to the presence of $CaCO_3$[13]. In general, the intensity for 50 wt. % and 30 wt. % CaO loading showed that the catalyst was mainly crystalline. Whereas, the XRD spectrum of the synthesized 10wt. % CaO/γ-Al_2O_3 shows very low and broad peaks indicating that the sample was mainly amorphous. The observed peaks were similar with the pure γ-Al_2O_3 calcined at relatively higher temperature ($> 400^{o}$C). This can be related to high specific surface area of synthesized catalyst. It also indicates that 10 wt. % CaO are highly dispersed on γ-Al_2O_3 surface and no sharp crystalline peaks corresponding to any of the 10wt. % CaO/γ-Al_2O_3 were observed. It can be concluded from XRD that calcium oxide is well dispersed as small clusters on γ-Al_2O_3. The diffraction pattern of peaks at $2\theta = 18.01^{o}$, 34.5^{o}, 47.5^{o} and 48.6^{o} correspond to calcium carbonate ($CaCO_3$)[13]. Table 4.2 shows the crystalline size of γ-Al_2O_3, 10 wt. %, 30 wt. % and 50 wt. % CaO/γ-Al_2O_3 catalyst values, 5.27, 2, 12229.25 and 21450.58 nm respectively. With these results it can be concluded that the XRD peaks are very low and broad peaks when the catalyst is smaller crystalline size.

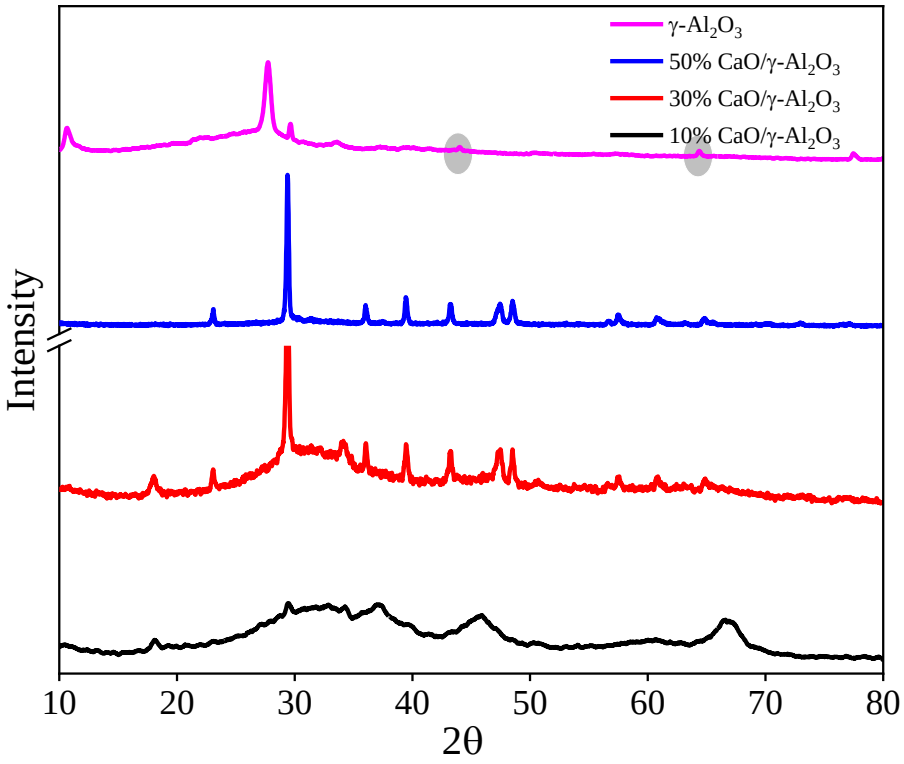

Figure 4.3: XRD patterns synthetized catalysts.

Table 4.2:- Percentage of Crystallinity and Crystallite size of catalysts.

Catalysts	Area of crystalline peaks	Area of all peaks	Crystallinity (%)	Crystallinity(nm)
γ-Al_2O_3	2052.92	4989	41.14	5.27
10%CaO/γAl_2O_3	789.92	1990	39.68	2
30%CaO/γAl_2O_3	1187.4	2760	43.7	12229.25
50%CaO/γAl_2O_3	1748.6	2891.6	60.47	21450.58

4.2.4. FTIR analysis

FT-IR spectrum of γ-Al_2O_3 powder is shown in Figure 4.4. The band at 547 cm^{-1} and 779 cm^{-1} are specifically marked out to -AlO_4 which indicates γ-Al_2O_3 contains octahedral and tetrahedral structure. This peak is attributed to the symmetric stretching vibrations of the Al–O–Al bonds [129]. It is in agreement with the FTIR spectrum of γ-alumina as reported elsewhere. The sets of bands detected from 3800 to 2700 cm^{-1} is imputed to -OH stretching in which its source may probably belong to the different chemical compounds. Broad stretching bend appeared at around 3400 cm^{-1} revealed the presence of hydroxyl group.

As shown in Figure 4.4 the band at 1669cm^{-1} was due the bending vibration of –OH in the presence of physisorbed water. The peaks in the 400-1000 cm^{-1} range (i.e. 547 and 779 cm^{-1}) has confirmed the formation of the γ-Al_2O_3 phase of alumina [130] as shown in Fig. 4.4. The other peaks in the region of 1520 cm^{-1} and 1316 cm^{-1} may be due to an impurity from urea and aluminum nitrate nonahydrate left in the gamma phase.

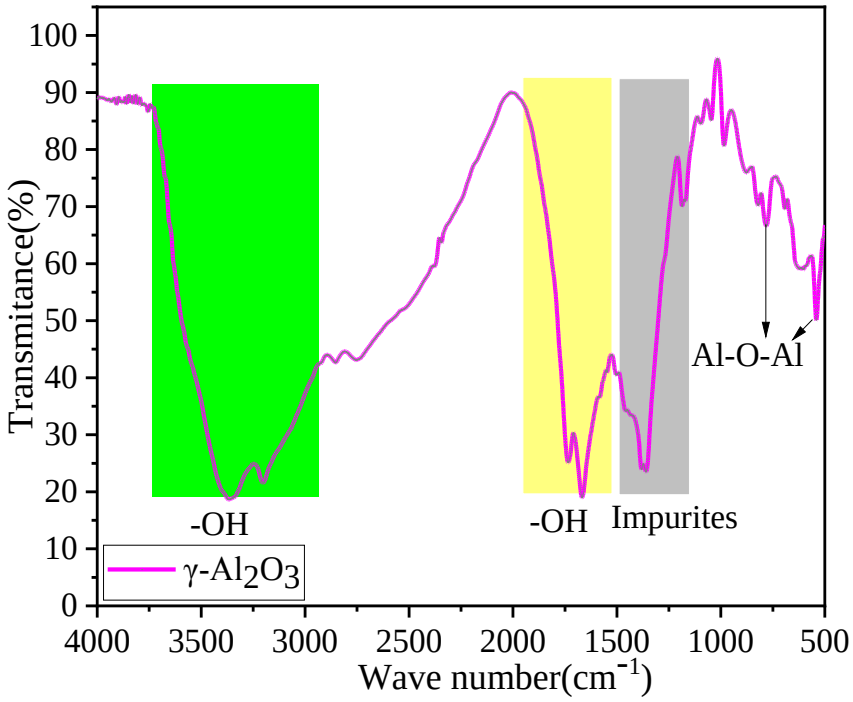

Figure 4.4: IR spectrum of γ-Al_2O_3 powder.

As shown in Figure 4.5: the bands centered at 876 cm^{-1} belongs to the bending vibrations of the Al–O–Al bonds[131]. Figure4.5 showed that the strong band at 1427cm^{-1} due to the presence of $CaCO_3$, which is mainly due to C-O band from incompletely decomposed carbonate in CaO/γ-Al_2O_3. The intensity of this band increases with the amount of catalyst loaded into γ-Al_2O_3 .The band in the region of 500 cm^{-1} i.e. 534 cm^{-1} and 875cm^{-1} imputed to CaO bond would really describe existence of CaO [132]. In this region, it was also observed that the intensity of this strong band increased with a decreased in wave length for all catalyst loading. This is mainly attributed with the presence of CaO in the catalyst which was proved already by XRD and SEMEDX. The intensity also increased with the amount of CaO loaded on γ-Al_2O_3. The small band centered at 2522 and 1779 cm^{-1} was ascribed by chemical absorption of CO_2, CO, CO_3^{2-}, or HCO_3^{1-}. Heating chemicals at temperature of 800°C does not guarantee the removal of these compounds as these are chemically absorbed inside either open or closed pores. The strong and intense band at

3643cm^{-1} corresponds to the O–H stretching vibration imputed to OH groups from calcium hydroxide.

As shown in Figure 4.5 manifold bands from 3800 to 2700 cm^{-1} is ascribed to OH stretching which has been brought into existence from various sources into the surface of the activated CaO/γ-Al_2O_3 i.e. mainly from absorbed moisture from the humid environment and the existed calcium hydroxide formed when CaO gets contacted with moisture[133]. However, the CaO/γ-Al_2O_3 catalysts showed intense and broad bands in the region of 1400-1600 cm^{-1} which revealed the existence of mono and bicarbonates[134]

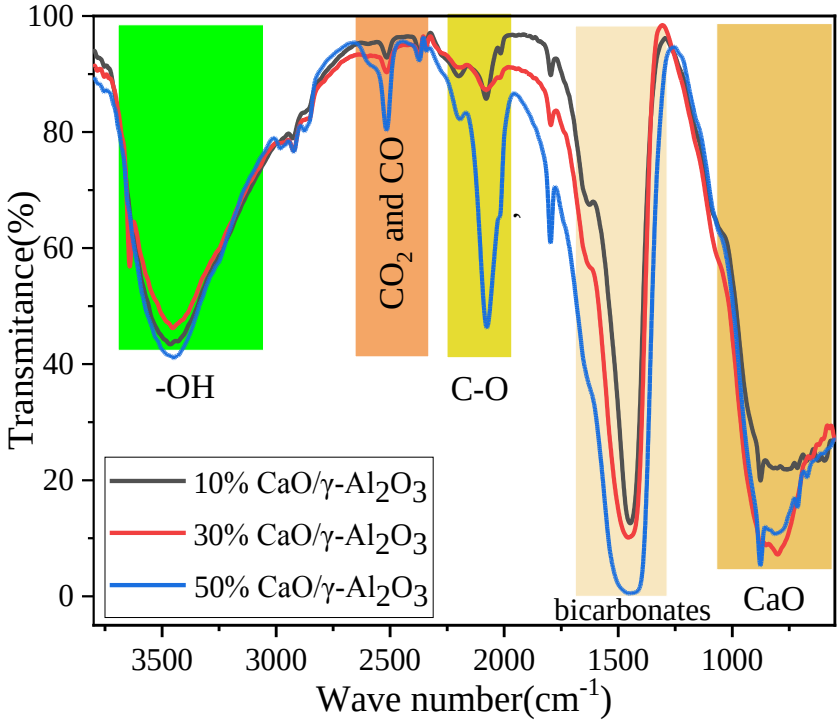

Figure 4.5: IR spectrum of a) 10 wt% b) 30 wt% and c) 50 wt% CaO/γ-Al_2O_3 powder.

4.3. Thermal decomposition of corn cob in the presence of CaO/ γ-Al_2O_3

Figure 4.6: shows the catalytic degradation of corn cob with γ-Al_2O_3, 10 wt%, 20 wt%, 30 wt%, 40 wt% and 50 wt% CaO loaded on γ-Al_2O_3 support were conducted. Thermal cracking of pure corn cob was also conducted for comparison.

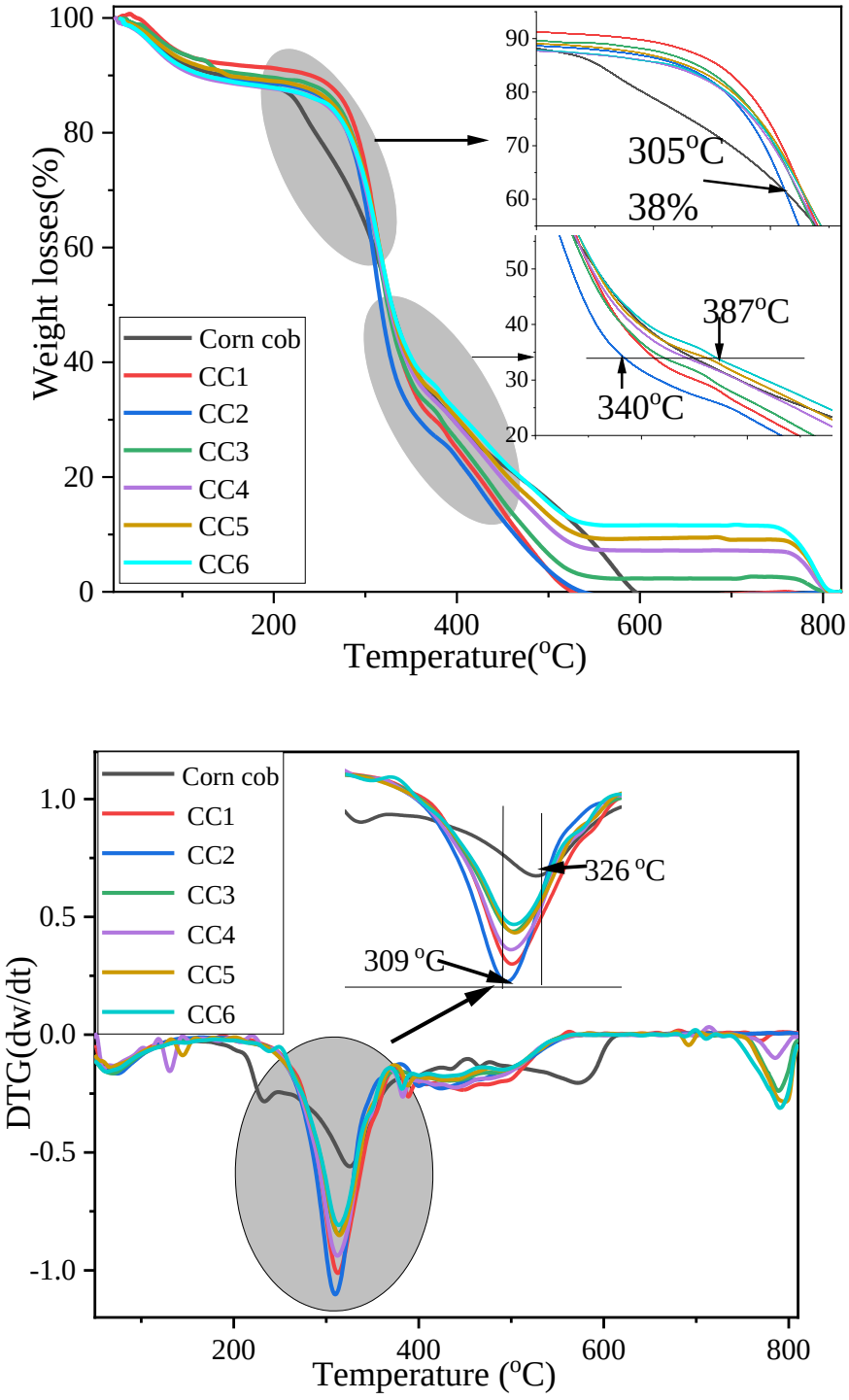

Figure 4.6: (a) The normalized mass loss (%) and (b) DTG (dw/dt) for all sample as function of temperature.

Thermal degradation of biomass is categorized into three stages such as dehydration, devolatization and carbonization. The first stage in thermal conversion corresponds to simple dehydration and it takes place in the temperature range of 25-275°C. Figure 4.6(a) show the moisture and light component content removed from the corn cob in presence of γ-Al_2O_3 (CC1), 10w.% CaO/γ-Al_2O_3 (CC2), 20 wt.% CaO/γ-Al_2O_3 (CC3), 30 wt.% CaO/γ-

Al_2O_3 (CC4), 40 wt.% CaO/γ-Al_2O_3(CC5)and 50 wt.% CaO/γ-Al_2O_3 (CC6). In DTG curve (Figure 4.6.b), this stages in the temperature range 25-250 ^oC significant temperature variation was not observed for all cases (CaO loading ratio on γ-Al_2O_3 support) with corn cob except decomposition of pure corn cob in the absence of catalyst

The second stage or intermediate step is devolatization, which take place in the temperature range of 275-490 ^oC. The summarized devolatization temperature of corn cob and all others samples (corn cob with catalyst at different ratio) were showed in Table 4. It was also observed that in figure 4.6 (a) and (b) the thermal degradation of corn cob and CC2 can be crossing each other at 39% and 305^oC. The normalized DTG curve was characterized by the formation of peaks at 326^oC, 312.9^oC, 309 ^oC, 314.5^oC, 312^oC, 314^oC and 315^oC for corn cob, CC1, CC2, CC3, CC4, CC5 and CC6 respectively. Therefore, the decomposition temperature of CC2 is lower than decomposition temperature of corn cob, CC1 and CC3-CC6. The final stage in corn cob thermal decomposition is carbonization, occurring at temperature range 490-780 ^oC. As observed in figure 4.6a, the final residues left, formed by the catalysts were 0 %, 0.442%, 0.45 %, 2.12%, 2.6%, 7.4%, 9.33% and 11.97% for the corn cob and CC1-CC6. The DTG curve above presented a small shoulder decreasing its amplitude with the temperature increasing, resembling a tail shape. This behaviour is due to the catalyst and minerals thermal decomposition which is characterized by low reaction rate and broad temperature range. In conclusion, it was observed that the higher CaO loading into γ-Al_2O_3 support, the higher mass percent remains as a residue. .From Figure 4.6 (a) the lowest reaction time and degradation temperature was observed that when 10wt. % of CaO/ γ-Al_2O_3 catalyst was used with corn cob as compared to all other cases mentioned above.

Table 4.3:- Summarized Thermo gravimetric analysis obtained from TGA and DTG for corn cob and corn cob with catalysts (γ-Al_2O_3, 10wt. %, 20wt. %, 30, 40 wt, %, and 50wt. % CaO/ γ-Al_2O_3)

	Corn cob	CC1	CC2	CC3	CC4	CC5	CC6
$T_{15}(^oC)$	220	270	245.6	258	230	230	251
$T_{Max}(^oC)$	326	312.9	309	314	312	315	313.5
$T_{95}(^oC)$	523.5	45	450	467	493	529	524

4.4. Effect of catalyst loading and heating rate

4.4.1. Effect of catalyst loading

The influence of catalyst weight loading on pyrolysis of corn cob was investigated. 10wt. % CaO loaded into γ-Al_2O_3 was selected based on its best performance of degradation as presented before. The weight loss and derivative thermogravimetric evaluation profiles were shown in Figure 4.4(a) and (b) for the catalytic degradation of corn cob with selected catalyst loading ratio. It is divided into three phase; phase I referred to moisture and light component evaluation that occurred at temperature below 250^oC, phase II referred as degradation of hemicellulose that attained at temperature range 250 to 450^oC and finally slow decomposition of lignin and catalyst (>700^oC), over a broader temperature range (450-770^oC) which can be denoted as phase III.

Table 4.4:- Catalytic degradation of corn cob at different catalyst loading.

	2% (CL)	4% (CL)	6% (CL)	8%(CL)
T_{15} (^oC)	276	261.65	261.2	261.43
T_{Max} (^oC)	311	312.24	309	314
T_{95} (^oC)	499	521.35	534	549

The results of phase I show that catalyst loading 2.wt% sample have achieved the removal temperature of moisture and light component at 276 ^oC. Catalysts loading of 2 wt. %, 4 wt. %, 6 wt. % and 8 wt. % samples were observed to have on almost similar temperature 261.2^oC up to 262.2^oC. Overall, based on Figure 4.7, the moisture removal temperature was evolved at less than > 5^oC for all investaged samples in the phase I. It is clearly stated that the influence of catalyst to corn cob ratio does play any significant role in the phase I.

After the phase I, the corn cob continues to degrade in phase II with more mass loss observed as it can be seen in Figure 4.7 (a) and (b) and the catalyst loading on the corn cobs that enhances the thermal degradation of cellulose-hemicellulose in the corn cob during pyrolysis. A phase II, among the entries investigate sample, 6 wt. % catalyst loading shows the promising results of achieving the lowest temperature that can contribute to reduce the cost of pyrolysis reactor. After the phase II, the corn cob continues to degrade in phase lignin and catalyst decompositions for (the temperature above 700^oC). Lignin is one of the major components of lignocellulosic structure that are found in the biomass materials. The Lignin components are only start to degrade at temperature above

than 490°C as plotted in Figure 4.7 (a) due to more complex structure than the hemicellulose and cellulose components.

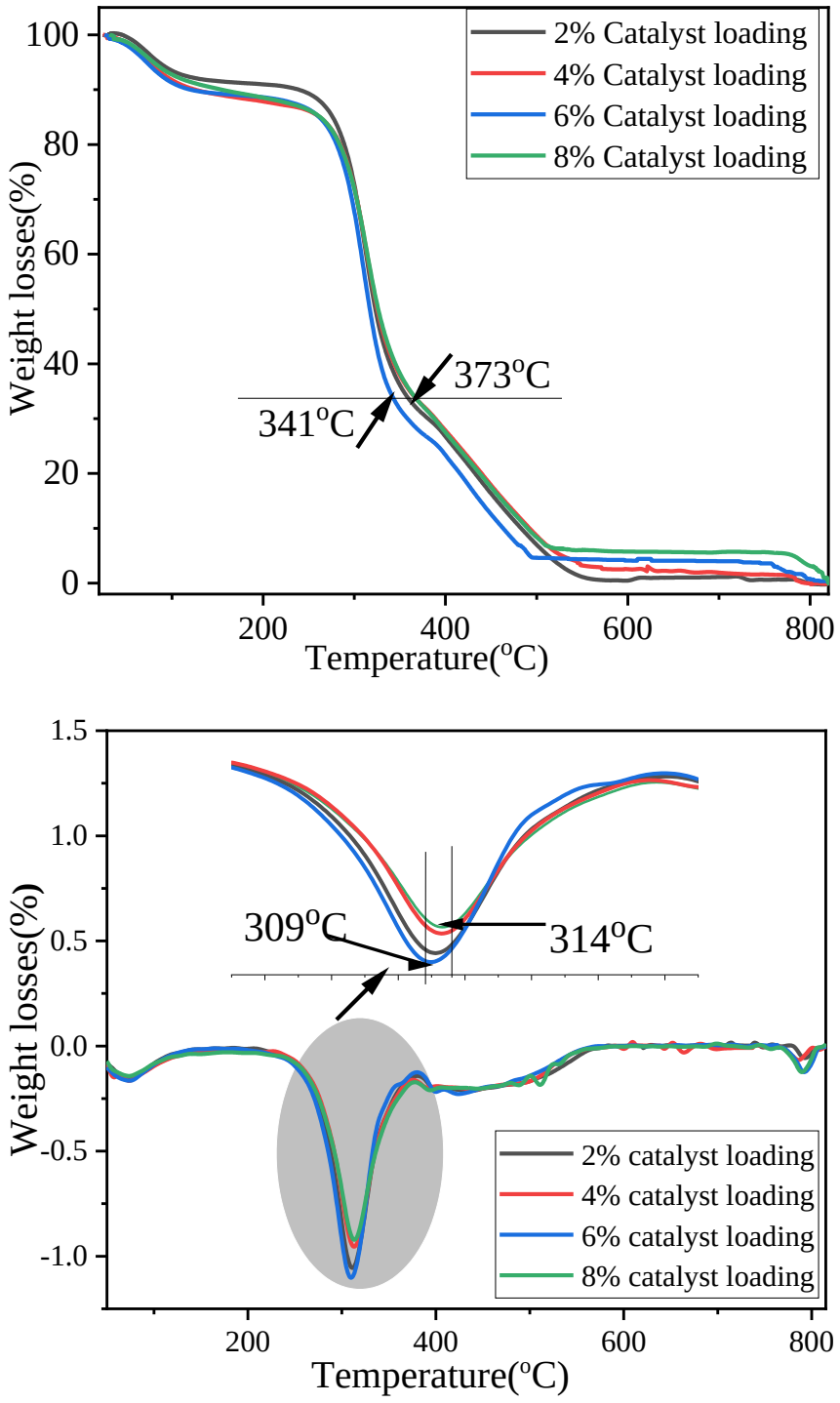

Figure 4.7: A part of TGA (a) and DTG (b) for 2 wt. % to 8 wt. % catalyst loading in the corn cob.

4.4.2. Effect of heating rate

Figure 4.8 shows the thermogravimetric analysis and derivative thermogravimetric analysis curves of corn cob pyrolysis at different heating rates of 5, 10, 15 and 20^{o}C/min form ambient to 900^{o}C. There were three distinct stages of weight loss at different heating rates; a dehydration stages (25-200^{o}C), a second active pyrolysis stages (200-500^{o}C) and passive pyrolysis stage (400-800^{o}C). During zone I the small changes in loss of the mass is attributed to the loss of water and light volatile compounds in the corn cob samples. In zone II is characterized by major mass loss, mainly from the decomposition of hemicellulose, cellulose and lignin which is in agreement with other biomass pyrolysis[104]. TGA curves (Figure 4.8a) of the corn cob samples exhibited two mass loss steps. A peak was observed in the DTA curve (Figure 4b); with the peak temperature at 340^{o}C and the rate of mass loss reaches its maximum. In this stage, most of the organic materials were gradually released, resulting in a large loss of mass (more than 70% of total volatiles) and the formation of the main pyrolytic products. During zone III, the carbonaceous matter decomposed at 5, 10, 15 and 20^{o}C/min heating is presented in table. The TGA curves showed that they shifted towards the right as heating rate increased. It generally follows a non- isothermal pyrolysis process. It can be seen form Figure 4.8 (b) that the rate of decomposition tends to increases as the heating rate increases because there is more thermal energy to facilitates better heat transfer between the surrounding and the inside of the samples; the higher heating rates provided less reaction time to form more volatile products. The temperature corresponding to the maximum mass loss increases with heating rate as shown in Table 4.5. i.e. 430^{o}C, 458^{o}C, 467.4^{o}C and 469.52^{o}C for 5, 10, 15 and 20^{o}C/min heating rates in order.

Table 4.5:- Peak temperatures and sample mass loss in the thermogravimetric test.

Heating rate (°C/min)	Zone II				Residue (%)
	Stage I (0.3-0.5)		stage II (0.51-0.9)		
	T_{max}(°C)	Mass loss(%)	T_{max}(°C)	Mass loss (%)	
5	290.29	50.12	430	90.77	2.48
10	311.12	52.2	458	90.89	3.08
15	332.13	54.35	467.4	91.12	4.82
20	349.16	55.75	469.52	91.24	4.52

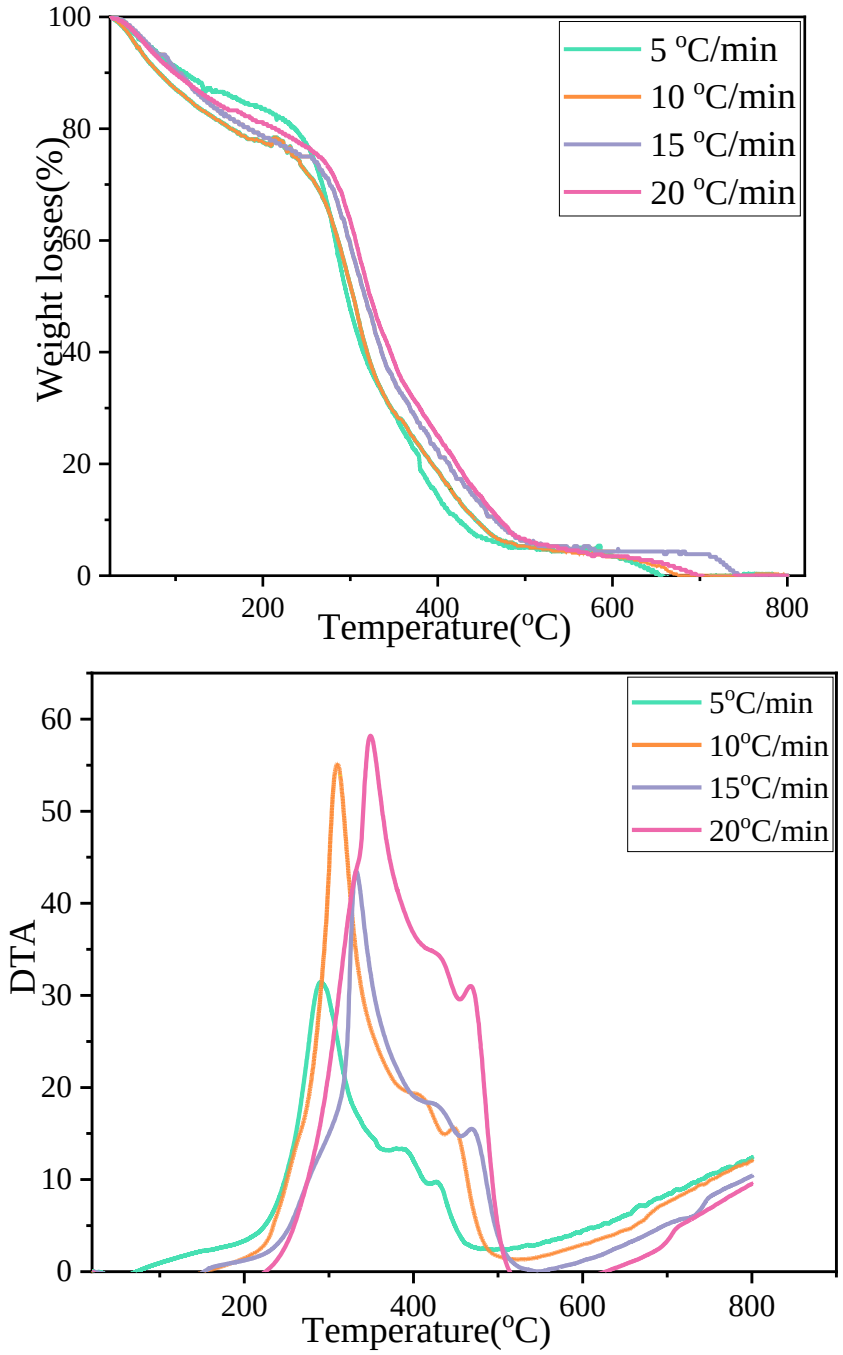

Figure 4.8: (a) TG and (b) DTA curves of corn cob at different heating rates.

4.5. Determination of kinetics parameters

Estimation of kinetic parameters involves activation energy and pre-exponential factor of the corn cob. The sample of corn cob has undergone non-isothermal temperature in the presence of nitrogen atmosphere. This study proposes different model-free methods and comparison with the integral method, i.e. Model based method (Coats-Redfern), FWO and KAS methods are used to determine kinetic parameters.

4.5.1. Calculation of activation energy

In this part, the activation energy and linear correlation coefficient at various conversion rates of 0.3–0.9 were calculated using the KAS and FWO methods. The kinetic parameters calculated using KAS method. The activation energy calculated using the decreased with increasing α in range of (0.3-0.5), (0.55-0.75) and (0.8-0.9). The FWO method is an integral method, which is also independent of the degradation mechanism. According to equation (2.13), numerous pairs of ln (β) and 1/T data at various conversion values of 0.3–0.9 were plotted and displayed in Figure 4.10. The activation energy were then calculated by the slopes (-0.457Eα/R) and listed in Table 4.7. Like the above method, this manifested a noticeable decreasing with increasing trends. The Eα values gradually decreased from 165.87kJ/mol to 129.186kJ/mol and 177.18 to 96.7kJ/mol with an increase in α from 0.3 to 0.5 and 0.55 to 0.8. Beyond this range (α >0.8) the Eα values increased slightly to 105.26 and 110.2kJ/mol for conversion values of 0.85 and 0.9, respectively. Therefore, the entire variation of Eα can be divided into region I (< 0.5), II (< 0.8) and region III (>0.8) according to the conversion rate. The average values of Eα were determined to be 138.89, 113.8 and 107.724 kJ/mol for regions I, II and III respectively. Comparing the two methods, higher R^2 values were derived from the FWO method for conversion (α) range of 0.3–0.9. Therefore, the FWO was the most reliable method and this was used for the reaction mechanism study in the following section.

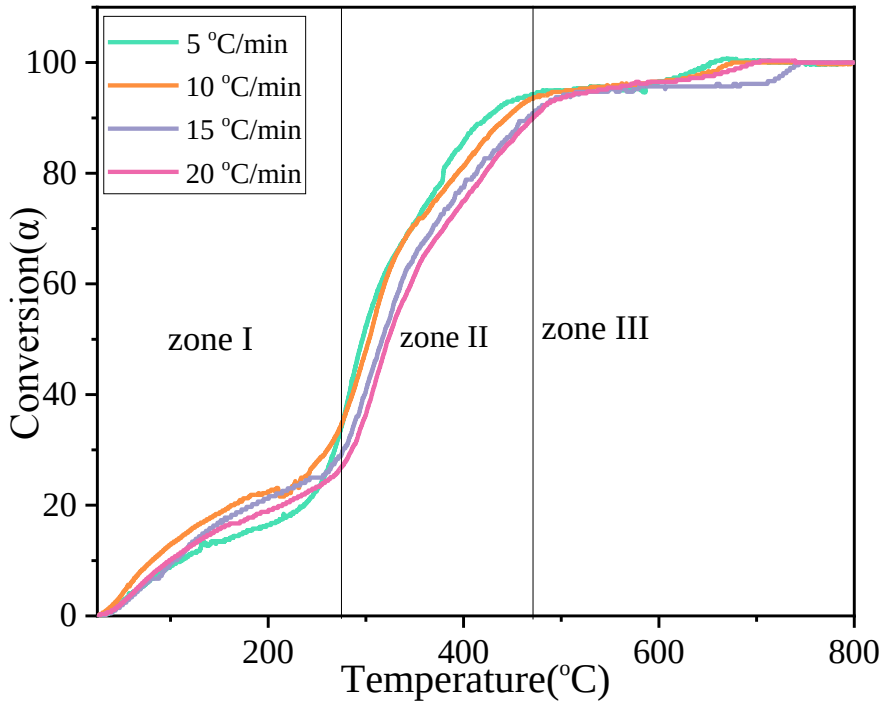

Figure 4.9:- Conversion rate curves of corn cob at different heating rates

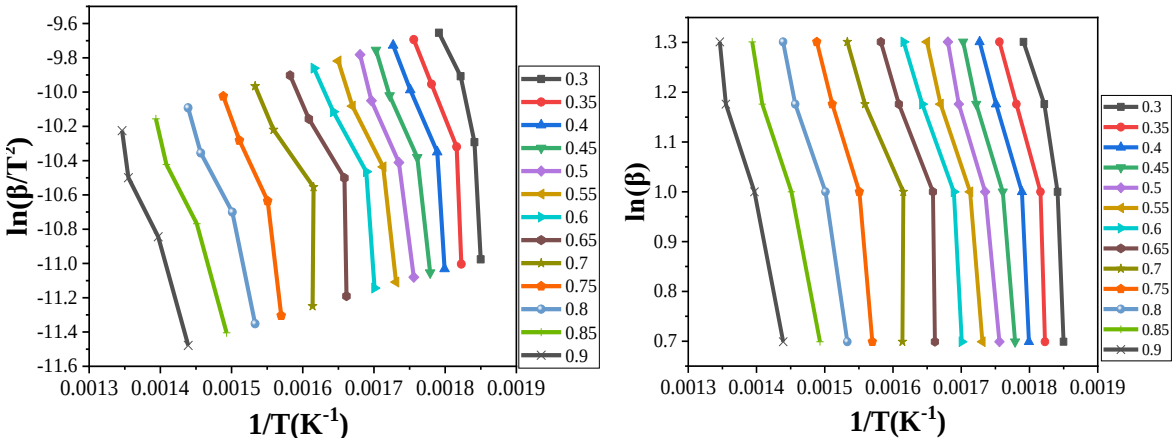

Figure 4.10: Kinetics analysis of catalytic pyrolysis of corn cob using KAS and FWO.

Table 4.6: The kinetic parameters determined using the FWO and KAS.

A	Flynn–Wall–Ozawa			Kissinger–Akahira–Sunose		
	E (kJ/mol)	LnA	R^2	E (kJ/mol)	LnA	R^2
0.3	165.014	17.60	0.8169	164.503	25.89	0.8
0.35	137.835	14.63	0.85	135.755	19.05	0.832
0.4	131.983	13.85	0.87	129.454	17.23	0.86
0.45	131.031	13.58	0.93	128.329	16.57	0.913
0.5	129.558	13.26	0.94	126.645	15.06	0.93
Average	138.89					
0.55	177.188	17.62	0.9637	176.700	25.82	0.95
0.6	110.844	11.17	0.8	106.614	10.91	0.84
0.65	109.318	10.82	0.869	104.793	10.07	0.7677
0.7	101.632	9.87	0.765	96.398	7.82	0.723
0.75	99.294	9.43	0.866	93.649	6.74	0.833
0.8	96.727	8.95	0.9181	90.601	5.125	0.8985
0.85	105.264	9.35	0.986	99.244	6.46	0.9818
0.9	110.182	9.43	0.9807	103.995	6.554	0.976
Average	113.8			109		

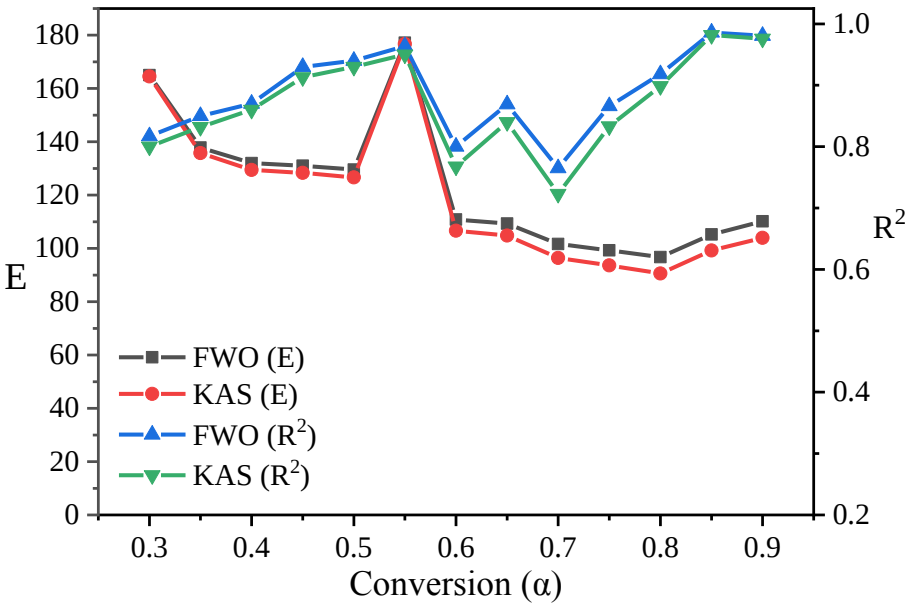

Figure 4.11: Comparison of kinetic parameters derived from KAS and FWO.

4.5.2. Estimation of reaction models

Employment of the Coat Redfern method for TG data can determine the most probable mechanism function and enable the pre-exponential factor(A) to be calculated [135], [136]. If the average Eα values for four heating rates based on a certain mechanism are comparable to the values from the FWO method, then this mechanism could be responsible for the reaction. From equation (3.9), the activation energy for all g (α) functions listed in Table 4.8 can be obtained. The resulting kinetic parameters are displayed in Figure 4.12. For each model, the Eα values decreased with the increase of heating rate. The Eα and R^2 values can be used as criteria for determining the most reliable reaction models. The conversion value range between 0.3-0.5 and 0.51-0.9, F6.5 and F4 model result average Eα values were 143.55 and 104.78 kJ/mol respectively. Therefore, the most appropriate mechanism for corn cob with 6% catalyst loading can be regarded to be the six half-order reaction (F6.5) and fourth-order reaction (F4) model [137].

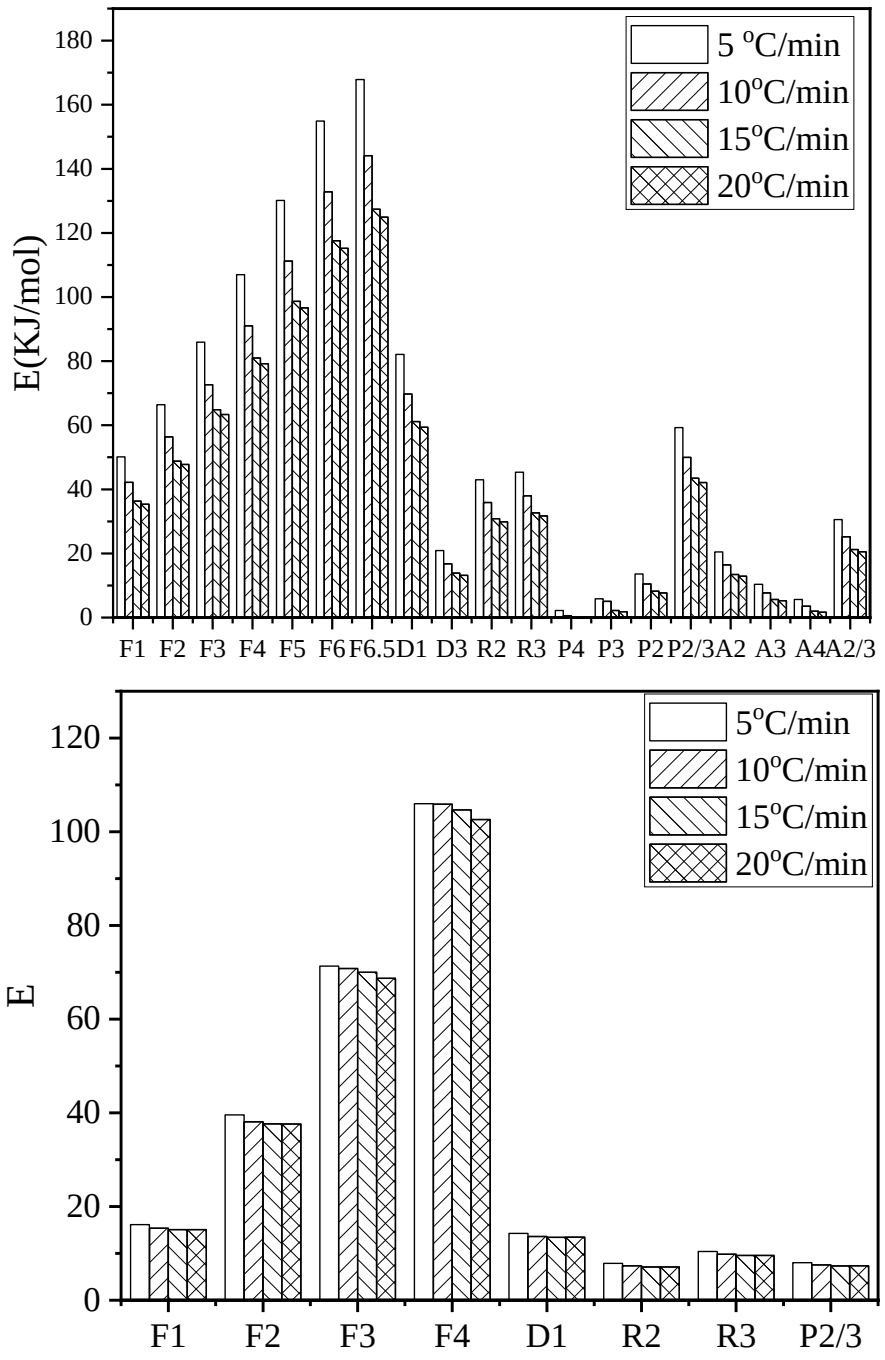

Figure 4.12: Comparison of kinetic parameters calculated from Coat-Redfern.

The curve fitting comparison between calculated TGA curve for reactions (F6.5and F4) of mechanism and experimental curve are shown in Figure 4.13. Also the initial temperature for all curves was considered to be same, but the reaction starts at different temperatures in simulated TGA curves. The range of reaction temperature for predicted TGA curve is in agreement with that of experimental work [138], [139].

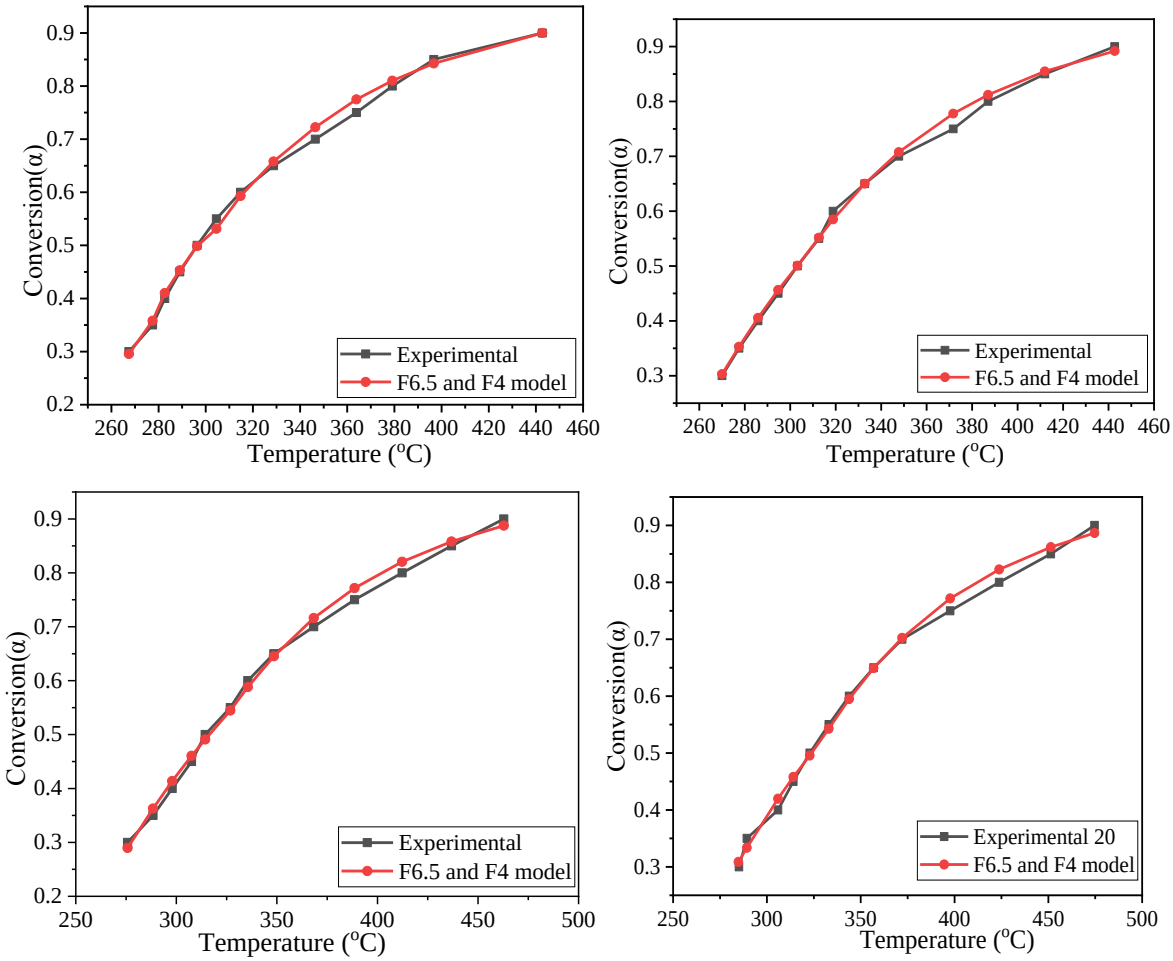

Figure 4.13: Curve fitting of corn cob pyrolysis using the kinetic data calculated from CR method (F6.5 and F4 model) for: (A) 5, (B) 10, (C) 20 and (D) 20°C/min.

Table 4.7: The kinetic parameters calculated using the Coat Redfern method.

Model	E (kJ/mol)		R^2	
	0.3-0.5	0.51-0.9	0.3-0.5	0.51-0.9
F1	41.964	16.242	0.9878	0.98006
F2	55.774	39.62	0.989	0.987275
F3	71.691	70.21	0.98762	0.976328
F4	89.564	104.78	0.98762	0.9795
F6.5	143.556	-	0.984225	-
D1	69.05	14.414	0.995	0.9261
D2	17.245	-2.32	0.99145	0.7
R2	35.92	7.99	0.994475	0.923
R3	37.813	10.54	0.6	0.955
P4	1.4	-7.43	0.9761	0.977
P3	4.97	-6.433	0.986675	0.979
P2	11.06	-4.311	0.986675	0.899
P2/3	49.893	8.2	0.985463	0.8402
A2	16.286	2.845	0.9814	0.83
A3	7.555	-1.71	0.945425	0.82
A4	3.447	-3.85	0.8945	0.971
A2/3	25.017	7.725	0.985475	0.954

4.5.3. Calculation of preexponential factors

The kinetic compensation effect is usually used to characterize the dependence of E and A on the conversion degree according to the following linear relationship[140].

Where, a and b are constants and refer to the compensation Coefficients.

$$\ln A = a + bE \quad \text{.....(4.1)}$$

The F6.5 and F4 mechanism were selected for determining the preexponential factors as a function of conversion to validate the kinetic parameter. The activation energy calculated using the FWO method was more reliable and was used in this section.

Substituting g (a) = $((1-\alpha)^{-6.5}-1)/$ (5.5) and g (a) = $((1-\alpha)^{-3}-1)/$ (3) into equation (4.3) yields

$$\ln(\beta) = -1.0518\left(\frac{E_\alpha}{RT}\right) + \ln\left(\frac{E_\alpha}{Rg(\alpha)}\right) - 5331 \quad \text{.....(4.2).}$$

From the Eα values determined using the FWO method in Table 4.6, the ln A values can be calculated according to equation (4.2). A linear relationship, ln A = 0.1181E - 1.8543 (R^2 = 0.9943) and ln A = 0.1041E - 0.781 (R^2 =0.9953), can be found through plotting ln A against E, as shown in Figure 4.14. It indicated that compensation effect existed between the apparent Eα and ln A during the pyrolysis of corn cob. The ln A fell into the range of 17.6–13.26 and 17.63-8.95 with α increasing from 0.3 to 0.5 and 0.51-0.9, which can be confirmed by Table 4.6. Therefore, the kinetic compensation effect was a valid alternative to demonstrating the interrelationship between the kinetic parameters ln A and E due to the impact of the experimental conditions on the determination of kinetic parameter.

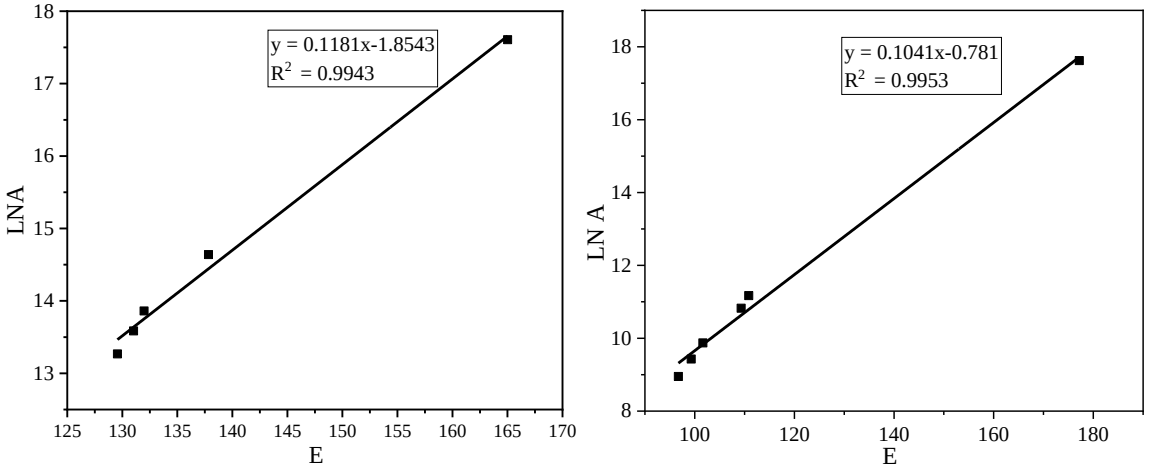

Figure 4.14: Compensation plot of lnA versus E

CHAPTER FIVE

5. CONCLUSION AND RECOMMENDATION

5.1. Conclusion

In this work, $CaO/\gamma\text{-}Al_2O_3$ solid heterogeneous catalyst which was prepared by the method of impregnation followed by drying in the oven and calcination at 700^{o}C for 4:30h in the furnace showed an excellent catalytic performance during thermal degradation of corn cob at 20 ^{o}C/min and. The synthesized $CaO/\gamma\text{-}Al_2O_3$ catalyst was characterized using XRD, FTIR, TGA and SEMEDX. It is confirmed that the catalysts (loaded with >10wt% CaO) possessed good thermal stability as per TGA analysis. The XRD pattern also confirmed that the catalyst selected (10wt% CaO/ $\gamma\text{-}Al_2O_3$) for catalytic decomposition of corn cob is mainly amorphous with low crystalline size (2nm).

In here, Thermal decomposition behavior and catalytic pyrolysis of corn cob were investigated using TGA. According to TGA and DTG curves, it was observed that the addition of the $10\%CaO/\gamma\text{-}Al_2O_3$ catalyst resulted in lower decomposition temperature as compared to pure biomass decomposition. This study also showed the effect of heating rate and catalyst to biomass ratio under non-isothermal conditions, in which the corn cob with $10\%CaO/\gamma\text{-}Al_2O_3$ sample was analyzed at four different constant heating rates of 5, 10, 15 and 20 °C/min. Hence, the increase in heating rate shifted the decomposition process to a higher temperature zone, but not very distinctly. Based on the TGA analysis, the activation energy and linear correlation coefficient were determined at different conversion rates using two model-free methods. From the DTG curve it was observed that the decomposition stages divided into two zones, which indicates the necessity of two different models. The KAS and FWO methods were used for the determination of kinetic reaction parameters. However, the Eα and R^2 values determined from KAS method fluctuated significantly. For a comparison, higher R^2 values were derived from the FWO method, which was the most reliable method used for the study of the reaction mechanism. Out of the CR methods, the F6.5 and F4 model gave higher R^2 values and also represent the first and second zone of the decomposition stage respectively. The calculated E values were comparable to the average values from the FWO method. The value of lnA was calculated based on the F6.5, F4 model and the FWO method and fell into the range 17.6–13.26 min^{-1} and 17.63-8.95 min^{-1} with α increasing from 0.3 to 0.5 and 0.51 to 0.9 respectively. The study of the kinetic compensation effect indicated that a compensation

effect existed between the apparent activation energy and the pre-exponential factor during the catalytic pyrolysis of corn cob.it was also observed that the proposed model fitted with the experimental results.

5.2. Recommendation

- Deep investigation and analysis is needed on the synthesis of 10 wt. % CaO/ γ-Al_2O_3 catalyst since it has shown unique performance and characteristics as compared to others.
- Further investigation is needed on the effect of catalyst on the bio oil composition and yield in addition to the thermal performance investigated in this work.
- Deeper kinetic study is needed to determine the kinetic parameters using optimization techniques or other techniques to perfectly fit the model with the experimental results.
- In the future, researchers may check the performances of 10 wt. % CaO/γ-Al_2O_3, as these had the best performance in this work. Also the obtained catalyst may be studied in catalysis of different processes or different biomass feedstocks.
- It is suggested that future work should focus on corn cob for design and optimization of the devolatilization section of reactors used in thermochemical processes.

REFERENCE

[1] J. Goldemberg, A. K. N. Reddy, K. R. Smith, and R. H. Williams, "Rural energy in developing countries," *World energy Assess. Energy Chall. Sustain.*, no. 10, pp. 367–384, 2000.

[2] F. A. O. F. Paper, "FORESTRY Key issues," 2018, Rome, 2018.

[3] A. Hameed, "Lignocellulosic Biomass : A Sustainable Bioenergy Source for Future Lignocellulosic Biomass : A Sustainable Bioenergy Source for the Future," *Lignocellul. Biomass A Sustain. Bioenergy Source Futur. Lignocellul. Biomass A Sustain. Bioenergy Source Futur.*, no. January, p. 17, 2018.

[4] UNEP, "Etiopia: Energy profile, Total energy production,Total energy consumption and Production," no. Table 1, pp. 2013–2016, 2015.

[5] A. S. Taffesse, P. Dorosh, and S. Asrat, "Crop production in Ethiopia : Regional patterns and trends Crop Production in Ethiopia : Regional Patterns and Trends," no. January 2013, 2017.

[6] S. Danje, "Fast pyrolysis of corn residues for energy production," no. December, pp. 1–222, 2011.

[7] N. Dewayanto and M. R. Nordin, "Catalytic Pyrolysis of Biomass to Synthesize Bio-oil and Chemicals: A Review," *Chem. J. Tek. Kim.*, vol. 2, no. 1, p. 29, 2016.

[8] T. S. Nguyen, "Development of an efficient catalyst for the pyrolytic coversion of biomass into transport fuel Tang Son Nguyen," vol. 1–146, 2014.

[9] V. Dhyani and T. Bhaskar, "A comprehensive review on the pyrolysis of lignocellulosic biomass," *Renew. Energy*, vol. 129, pp. 695–716, 2018.

[10] A. Sharma, V. Pareek, and D. Zhang, "Biomass pyrolysis - A review of modelling, process parameters and catalytic studies," *Renew. Sustain. Energy Rev.*, vol. 50, pp. 1081–1096, 2015.

[11] D. Tapasvi, R. Khalil, G. Várhegyi, K. Q. Tran, M. Grønli, and Ø. Skreiberg, "Thermal decomposition kinetics of woods with an emphasis on torrefaction," *Energy and Fuels*, vol. 27, no. 10, pp. 6134–6145, 2013.

[12] S. Vyazovkin *et al.*, "ICTAC Kinetics Committee recommendations for collecting experimental thermal analysis data for kinetic computations," *Thermochim. Acta*, vol. 590, pp. 1–23, 2014.

[13] M. Kaur and A. Ali, "Ethanolysis of waste cottonseed oil over lithium impregnated calcium oxide: Kinetics and reusability studies," *Renew. Energy*, vol. 63, pp. 272–

279, 2014.

[14] R. Ebrahimi Kahrizsangi, M. H. Abbasi, and A. Saidi, “Model-fitting approach to kinetic analysis of non-isothermal oxidation of molybdenite,” *Iran. J. Chem. Chem. Eng.*, vol. 26, no. 2, pp. 119–123, 2007.

[15] F. A. López *et al.*, “Kinetics of the Thermal Degradation of Granulated Scrap Tyres : a Model-free Analysis,” vol. 19, no. 4, 2013.

[16] M. Hussain, H. Zabiri, L. D. Tufa, and S. Yusup, “A Kinetic Study and Thermal Decomposition Characteristics of Palm Kernel Shell Using Model- fitting and Model-free Methods,” *Biofuels*, vol. 0, no. 0, pp. 1–12, 2019.

[17] R. M. B. Moreno, E. S. De Medeiros, F. C. Ferreira, N. Alves, and P. S. Gonc, “Thermogravimetric studies of decomposition kinetics of six different IAC Hevea rubber clones using Flynn – Wall – Ozawa approach,” vol. 35, no. 1, pp. 15–21, 2006.

[18] K. Raj, G. Burra, and A. K. Gupta, “Modeling of biomass pyrolysis kinetics using sequential multi-step reaction model,” *Fuel*, vol. 237, no. May 2018, pp. 1057–1067, 2019.

[19] P. Das and P. Tiwari, “Thermochimica Acta Thermal degradation kinetics of plastics and model selection,” *Thermochim. Acta*, vol. 654, no. May, pp. 191–202, 2017.

[20] A. W. Coats and J. P. Redfern, “Kinetic parameters from thermogravimetric data [12],” *Nature*, vol. 201, no. 4914, pp. 68–69, 1964.

[21] J. Aguado, D. P. Serrano, G. S. Miguel, J. M. Escola, and J. M. Rodríguez, “Catalytic activity of zeolitic and mesostructured catalysts in the cracking of pure and waste polyolefins,” *J. Anal. Appl. Pyrolysis*, vol. 78, no. 1, pp. 153–161, 2007.

[22] A. K. Panda, R. K. Singh, and D. K. Mishra, “Thermolysis of waste plastics to liquid fuel. A suitable method for plastic waste management and manufacture of value added products-A world prospective,” *Renew. Sustain. Energy Rev.*, vol. 14, no. 1, pp. 233–248, 2010.

[23] A. Coelho, L. Costa, M. M. Marques, I. M. Fonseca, M. A. N. D. A. Lemos, and F. Lemos, “The effect of ZSM-5 zeolite acidity on the catalytic degradation of high-density polyethylene using simultaneous DSC/TG analysis,” *Appl. Catal. A Gen.*, vol. 413–414, pp. 183–191, 2012.

[24] D. W. Park, E. Y. Hwang, J. R. Kim, J. K. Choi, Y. A. Kim, and H. C. Woo, “Catalytic degradation of polyethylene over solid acid catalysts,” *Polym. Degrad.*

Stab., vol. 65, no. 2, pp. 193–198, 1999.

[25] D. Version, *Improving the energy system for a rural community in developing countries Improving the energy system for a rural community in developing countries Challenges and sustainable opportunities in using renewable*. 2016.

[26] R. Kempener, O. Lavagne, D. Saygin, J. Skeer, S. Vinci, and D. Gielen, "Off-Grid Renewable Energy Systems: Status and Methodological Issues," *Irena*, p. 29, 2015.

[27] R. E. Guedes, A. S. Luna, and A. R. Torres, "Journal of Analytical and Applied Pyrolysis Operating parameters for bio-oil production in biomass pyrolysis : A review," *J. Anal. Appl. Pyrolysis*, vol. 129, no. November 2017, pp. 134–149, 2018.

[28] A. V. Bridgwater and G. V. C. Peacocke, "Fast pyrolysis processes for biomass," *Renew. Sustain. energy Rev.*, vol. 4, no. 1, pp. 1–73, 2000.

[29] D. S. Achilias, C. Roupakias, P. Megalokonomos, A. A. Lappas, and V. Antonakou, "Chemical recycling of plastic wastes made from polyethylene (LDPE and HDPE) and polypropylene (PP)," *J. Hazard. Mater.*, vol. 149, no. 3, pp. 536–542, 2007.

[30] R. L. White, "Acid-Catalyzed Cracking of Polyolefins: Primary Reaction Mechanisms," *Feed. Recycl. Pyrolysis Waste Plast. Convert. Waste Plast. into Diesel Other Fuels*, pp. 43–72, 2006.

[31] L. Kerkeni *et al.*, "We are IntechOpen , the world ' s leading publisher of Open Access books Built by scientists , for scientists TOP 1 %," *Intech*, no. tourism, p. 13, 2016.

[32] B. P. I. Guide, "Biomass Properties and Handling," pp. 1–27, 2011.

[33] W. U. K. Tareen *et al.*, "Present status and potential of biomass energy in pakistan based on existing and future renewable resources," *Sustain.*, vol. 12, no. 1, 2020.

[34] P. Fraenkel, S. Bailey, L. Bosselaar, and E. Larson, "Renewable energy technology," *Ind. Biotechnol.*, vol. 2, no. 4, pp. 276–295, 2006.

[35] G. Cavalaglio *et al.*, "Characterization of various biomass feedstock suitable for small-scale energy plants as preliminary activity of biocheaper project," *Sustain.*, vol. 12, no. 16, pp. 1–10, 2020.

[36] F. H. Isikgor and C. R. Becer, "Lignocellulosic biomass: a sustainable platform for the production of bio-based chemicals and polymers," *Polym. Chem.*, vol. 6, no. 25, pp. 4497–4559, 2015.

[37] A. Anca-Couce, *Reaction mechanisms and multi-scale modelling of lignocellulosic biomass pyrolysis*, vol. 53, no. March 2016. 2016.

[38] J. Yu, N. Paterson, J. Blamey, and M. Millan, "Cellulose , xylan and lignin

interactions during pyrolysis of lignocellulosic biomass," *Fuel*, vol. 191, pp. 140–149, 2017.

[39] K. S. Rawat, "BIOMASS TO FUEL : CONVERSION TECHNIQUES," no. June, 2016.

[40] D. Mohan, C. U. Pittman, and P. H. Steele, "Pyrolysis of Wood / Biomass for Bio-oil : A Critical Review," no. 4, pp. 848–889, 2006.

[41] O. Obafemi, A. Stephen, O. Ajayi, and P. Mashinini, "Experimental investigation of thermal properties of Lignocellulosic biomass : A review Experimental investigation of Lignocellulosic biomass : A review thermal properties of," *hermal Prop.*, vol. 1, pp. 6–7, 2018.

[42] S. Mandal, R. Bandyopadhyay, and A. K. Das, "Thermo-catalytic process for conversion of lignocellulosic biomass to fuels and chemicals : a review," vol. 3, no. 2, pp. 58–69, 2018.

[43] Y. Sun and J. Cheng, "Hydrolysis of lignocellulosic materials for ethanol production : a review q," *Bioresour. Technol.*, vol. 83, pp. 1–11, 2002.

[44] T. A. Maung and C. R. Gustafson, "Economic Impact of Harvesting Corn Stover under Time Constraint: The Case of North Dakota," *Econ. Res. Int.*, vol. 2013, pp. 1–13, 2013.

[45] L. N. Tandzi and C. S. Mutengwa, "Estimation of Maize (Zea mays L.) Yield Per Harvest Area: Appropriate methods," *Agronomy*, vol. 10, no. 1, pp. 1–18, 2020.

[46] A. Mohammed, "Ethiopia commodity exchange: Marketing prospects and challenges in focus," *African J. Mark. Manag.*, vol. 9, no. 3, pp. 18–24, 2017.

[47] D. Mejía, *Post-harvest Operations*, vol. 1. 2003, pp. 1–99.

[48] Y. Zhang, A. E. Ghaly, and B. Li, "Physical properties of corn residues," *Am. J. Biochem. Biotechnol.*, vol. 8, no. 2, pp. 44–53, 2012.

[49] P. Kumar, D. M. Barrett, M. J. Delwiche, and P. Stroeve, "Methods for pretreatment of lignocellulosic biomass for efficient hydrolysis and biofuel production," *Ind. Eng. Chem. Res.*, vol. 48, no. 8, pp. 3713–3729, 2009.

[50] T. Kan, V. Strezov, and T. J. Evans, "Lignocellulosic biomass pyrolysis : A review of product properties and effects of pyrolysis parameters," *Renew. Sustain. Energy Rev.*, vol. 57, pp. 1126–1140, 2016.

[51] P. Basu, *Biomass Gasification and Pyrolysis*. 2010.

[52] H. B. Goyal, D. Seal, and R. C. Saxena, "Bio-fuels from thermochemical conversion of renewable resources: A review," *Renew. Sustain. Energy Rev.*, vol.

12, no. 2, pp. 504–517, 2008.

[53] J. A. Caballero, R. Font, A. Marcilla, and J. A. Conesa, “New Kinetic Model for Thermal Decomposition of Heterogeneous Materials,” *Ind. Eng. Chem. Res.*, vol. 34, no. 3, pp. 806–812, 1995.

[54] N. P. Niemelä, H. Tolvanen, T. Saarinen, A. Leppänen, and T. Joronen, “CFD based reactivity parameter determination for biomass particles of multiple size ranges in high heating rate devolatilization,” *Energy*, vol. 128, pp. 676–687, 2017.

[55] L. Gašparovič, Z. Koreňová, and Ľ. Jelemenský, “Kinetic study of wood chips decomposition by TGA,” *Chem. Pap.*, vol. 64, no. 2, pp. 174–181, 2010.

[56] K. Werner, L. Pommer, and M. Broström, “Thermal decomposition of hemicelluloses,” *J. Anal. Appl. Pyrolysis*, vol. 110, no. 1, pp. 130–137, 2014.

[57] A. V. Bridgwater, “Renewable fuels and chemicals by thermal processing of biomass,” *Chem. Eng. J.*, vol. 91, no. 2–3, pp. 87–102, 2003.

[58] A. K. Varma, R. Shankar, and P. Mondal, *A Review on Pyrolysis of Biomass and the Impacts of Operating Conditions on Product Yield, Quality, and Upgradation*. 2018.

[59] E. Amini, M. S. Safdari, J. T. DeYoung, D. R. Weise, and T. H. Fletcher, “Characterization of pyrolysis products from slow pyrolysis of live and dead vegetation native to the southern United States,” *Fuel*, vol. 235, no. August 2018, pp. 1475–1491, 2019.

[60] H. Rate, “Principles of Pyrolysis,” in *TNAU Agritech Portal*, vol. 1, 2015, pp. 1–8.

[61] Y. Wang, “Catalytic fast pyrolysis of lignocellulosic biomass,” vol. 43, no. 22, 2014.

[62] L. Zajec, “Slow pyrolysis in a rotary kiln reactor : Optimization and experiment Luka Zajec Slow pyrolysis in a rotary kiln reactor :,” vol. 1, no. 1, pp. 30–50, 2009.

[63] T. Cornelissen, J. Yperman, G. Reggers, S. Schreurs, and R. Carleer, “Flash co-pyrolysis of biomass with polylactic acid. Part 1: Influence on bio-oil yield and heating value,” *Fuel*, vol. 87, no. 7, pp. 1031–1041, 2008.

[64] T. Hosoya, H. Kawamoto, and S. Saka, “Pyrolysis behaviors of wood and its constituent polymers at gasification temperature,” *J. Anal. Appl. Pyrolysis*, vol. 78, no. 2, pp. 328–336, 2007.

[65] M. Van de Velden, J. Baeyens, A. Brems, B. Janssens, and R. Dewil, “Fundamentals, kinetics and endothermicity of the biomass pyrolysis reaction,” *Renew. Energy*, vol. 35, no. 1, pp. 232–242, 2010.

[66] L. Axelsson, M. Franzén, M. Ostwald, G. Berndes, G. Lakshmi, and N. H. Ravindranath, "Perspective: Jatropha cultivation in southern India: Assessing farmers' experiences," *Biofuels, Bioprod. Biorefining*, vol. 6, no. 3, pp. 246–256, 2012.

[67] T. E. McGrath, W. G. Chan, and R. Hajajigol, "Low temperature mechanism for the formation of polycyclic aromatic hydrocarbons from the pyrolysis of cellulose. Journal of Analytical and Applied Pyrolysis, v. 66, p. 51-70, 2003.," *J. Anal. Appl. Pyrolysis*, vol. 66, pp. 51–70, 2003.

[68] J. L. Banyasz, S. Li, J. Lyons-Hart, and K. H. Shafer, "Gas evolution and the mechanism of cellulose pyrolysis," *Fuel*, vol. 80, no. 12, pp. 1757–1763, 2001.

[69] J. Scheirs, G. Camino, and W. Tumiatti, "Overview of water evolution during the thermal degradation of cellulose," *Eur. Polym. J.*, vol. 37, no. 5, pp. 933–942, 2001.

[70] A. M. Azeez, D. Meier, and J. Odermatt, "Temperature dependence of fast pyrolysis volatile products from European and African biomasses," *J. Anal. Appl. Pyrolysis*, vol. 90, no. 2, pp. 81–92, 2011.

[71] L. Wei *et al.*, "Characteristics of fast pyrolysis of biomass in a free fall reactor," *Fuel Process. Technol.*, vol. 87, no. 10, pp. 863–871, 2006.

[72] P. Morf, P. Hasler, and T. Nussbaumer, "Mechanisms and kinetics of homogeneous secondary reactions of tar from continuous pyrolysis of wood chips," *Fuel*, vol. 81, no. 7, pp. 843–853, 2002.

[73] R. J. Evans and T. a Milne, "Molecular characterization of pyrolysis of biomass. 1. Fundamentals," *Energy & Fuels*, vol. 1, no. 2, pp. 123–138, 1987.

[74] D. Neves, H. Thunman, A. Matos, L. Tarelho, and A. Gómez-Barea, "Characterization and prediction of biomass pyrolysis products," *Prog. Energy Combust. Sci.*, vol. 37, no. 5, pp. 611–630, 2011.

[75] H. E. Kissinger, "Reaction Kinetics in Differential Thermal Analysis," *Anal. Chem.*, vol. 29, no. 11, pp. 1702–1706, 1957.

[76] T. Ozawa, "Estimation of activation energy by isoconversion methods," *Thermochim. Acta*, vol. 203, no. C, pp. 159–165, 1992.

[77] N. Sbirrazzuoli, "Advanced isoconversional kinetic analysis for the elucidation of complex reaction mechanisms: A new method for the identification of rate-limiting steps," *Molecules*, vol. 24, no. 9, 2019.

[78] T. Ozawa, "A New Method of Analyzing Thermogravimetric Data," *Bull. Chem. Soc. Jpn.*, vol. 38, no. 11, pp. 1881–1886, 1965.

[79] A. C. R. Lim, B. L. F. Chin, Z. A. Jawad, and K. L. Hii, “Kinetic Analysis of Rice Husk Pyrolysis Using Kissinger-Akahira-Sunose (KAS) Method,” *Procedia Eng.*, vol. 148, pp. 1247–1251, 2016.

[80] S. Vyazovkin, A. K. Burnham, J. M. Criado, L. A. Pérez-Maqueda, C. Popescu, and N. Sbirrazzuoli, “ICTAC Kinetics Committee recommendations for performing kinetic computations on thermal analysis data,” *Thermochim. Acta*, vol. 520, no. 1–2, pp. 1–19, 2011.

[81] D. Almeida and M. D. F. Marques, “Thermal and catalytic pyrolysis of plastic waste,” vol. 26, no. 1, pp. 44–51, 2016.

[82] B. R. Goldsmith, B. Peters, J. K. Johnson, B. C. Gates, and S. L. Scott, “Beyond Ordered Materials: Understanding Catalytic Sites on Amorphous Solids,” *ACS Catal.*, vol. 7, no. 11, pp. 7543–7557, 2017.

[83] NPTEL, “Lecture 5 Solid catalysts,” *NPTEL – Chem. Eng. – Catal. Sci. Technol. Lect.*, pp. 1–53, 2014.

[84] J. C. Védrine, “Acid-base characterization of heterogeneous catalysts: An up-to-date overview,” *Res. Chem. Intermed.*, vol. 41, no. 12, pp. 9387–9423, 2015.

[85] G. P. Poduval, *On the role of acidity in amorphous silica-alumina based catalysts*, no. april. 2001.

[86] A. Arjah, “Catalytic Cracking of Pentene to Ethene and Propene Over ZSM-5 Zeolite,” 2019.

[87] K. P. Shadangi and K. Mohanty, “Thermal and catalytic pyrolysis of Karanja seed to produce liquid fuel,” *Fuel*, vol. 115, no. July, pp. 434–442, 2014.

[88] I. Y. Mohammed, F. K. Kazi, S. Yusup, P. A. Alaba, Y. M. Sani, and Y. A. Abakr, “Catalytic intermediate pyrolysis of Napier grass in a fixed bed reactor with ZSM-5, HZSM-5 and zinc-exchanged zeolite-a as the catalyst,” *Energies*, vol. 9, no. 4, 2016.

[89] Q. Lu, Z. Zhang, C. Dong, and X. Zhu, “Catalytic Upgrading of Biomass Fast Pyrolysis Vapors with Nano Metal Oxides: An Analytical Py-GC/MS Study,” pp. 1805–1820, 2010.

[90] D. J. Mihalcik, C. A. Mullen, and A. A. Boateng, “Journal of Analytical and Applied Pyrolysis Screening acidic zeolites for catalytic fast pyrolysis of biomass and its components ☪,” *J. Anal. Appl. Pyrolysis*, vol. 92, no. 1, pp. 224–232, 2011.

[91] J. C. Serrano-ruiz and J. A. Dumesic, “Catalytic Production of Liquid Hydrocarbon

Transportation Fuels," *Catal. Prod. Liq. Hydrocarb. Transp. Fuels*, pp. 29–56, 2012.

[92] A. Imran, E. A. Bramer, K. Seshan, and G. Brem, "An overview of catalysts in biomass pyrolysis for production of biofuels," *Biofuel Res. J.*, vol. 5, no. 4, pp. 872–885, 2018.

[93] M. M. Rahman, R. Liu, and J. Cai, "Catalytic fast pyrolysis of biomass over zeolites for high quality bio-oil – A review," *Fuel Process. Technol.*, vol. 180, no. August, pp. 32–46, 2018.

[94] S. D. Stefanidis, K. G. Kalogiannis, E. F. Iliopoulou, A. A. Lappas, and P. A. Pilavachi, "Bioresource Technology In-situ upgrading of biomass pyrolysis vapors : Catalyst screening on a fixed bed reactor," *Bioresour. Technol.*, vol. 102, no. 17, pp. 8261–8267, 2011.

[95] K. Ishaq, A. A. Saka, A. O. Kamardeen, A. Abdulrahman, I. K. Adekunle, and A. S. Afolabi, "Application of γ-alumina as catalyst support for the synthesis of CNTs in a CVD reactor," *Adv. Nat. Sci. Nanosci. Nanotechnol.*, vol. 9, no. 3, 2018.

[96] A. Eliassi and M. Ranjbar, "Application of Novel Gamma Alumina Nano Structure for Preparation of Dimethyl ether from Methanol," *Int. J. Nanosci. Nanotechnol.*, vol. 10, no. 1, pp. 13–26, 2014.

[97] S. Siahpoosh, E. Salahi, F. Hessari, and I. Mobasherpour, "Synthesis of γ-Alumina Nanoparticles with High-Surface-Area via Sol-Gel Method and their Performance for the Removal of Nickel from Aqueous Solution," *Bull. la Société R. des Sci. Liège*, pp. 912–934, 2016.

[98] J. Wang, Z. Zhong, Z. Song, K. Ding, and A. Deng, "Modification and regeneration of HZSM-5 catalyst in microwave assisted catalytic fast pyrolysis of mushroom waste," *Energy Convers. Manag.*, vol. 123, pp. 29–34, 2016.

[99] L. Ding, P. Rahimi, R. Hawkins, S. Bhatt, and Y. Shi, "Naphthenic acid removal from heavy oils on alkaline earth-metal oxides and ZnO catalysts," *Appl. Catal. A Gen.*, vol. 371, no. 1–2, pp. 121–130, 2009.

[100] K. P. Shadangi and K. Mohanty, "Thermal and catalytic pyrolysis of Karanja seed to produce liquid fuel," *Fuel*, vol. 115, pp. 434–442, 2014.

[101] A. Veses *et al.*, "Bioresource Technology Catalytic pyrolysis of wood biomass in an auger reactor using calcium-based catalysts," *Bioresour. Technol.*, vol. 162, pp. 250–258, 2014.

[102] R. Mahadevan, R. Shakya, S. Neupane, and S. Adhikari, "Physical and chemical

properties and accelerated aging test of bio-oil produced from in situ catalytic pyrolysis in a bench-scale fluidized-bed reactor," *Energy and Fuels*, vol. 29, no. 2, pp. 841–848, 2015.

[103] A. Imran, E. A. Bramer, K. Seshan, and G. Brem, "An overview of catalysts in biomass pyrolysis for production of biofuels," vol. 20, pp. 872–885, 2018.

[104] T. Mani, P. Murugan, J. Abedi, and N. Mahinpey, "Chemical Engineering Research and Design Pyrolysis of wheat straw in a thermogravimetric analyzer : Effect of particle size and heating rate on devolatilization and estimation of global kinetics," *Chem. Eng. Res. Des.*, vol. 88, no. 8, pp. 952–958, 2010.

[105] A. Ahmed *et al.*, "Effect of particle size on thermal decomposition and devolatilization kinetics of melon seed shell of melon seed shell," *Chem. Eng. Commun.*, vol. 0, no. 0, pp. 1–13, 2019.

[106] X. Yao, K. Xu, and Y. Liang, "Assessing the effects of different process parameters on the pyrolysis behaviors and Thermal Dynamics of corncob fractions," *BioResources*, vol. 12, no. 2, pp. 2748–2767, 2017.

[107] A. Veses, M. Aznar, J. M. López, M. S. Callén, R. Murillo, and T. García, "Production of upgraded bio-oils by biomass catalytic pyrolysis in an auger reactor using low cost materials," *Fuel*, vol. 141, pp. 17–22, 2015.

[108] X. Chen, Y. Chen, H. Yang, W. Chen, X. Wang, and H. Chen, "Fast pyrolysis of cotton stalk biomass using calcium oxide," *Bioresour. Technol.*, vol. 233, pp. 15–20, 2017.

[109] S. H. Russell, J. L. Turrion-Gomez, W. Meredith, P. Langston, and C. E. Snape, "Increased charcoal yield and production of lighter oils from the slow pyrolysis of biomass," *J. Anal. Appl. Pyrolysis*, vol. 124, pp. 536–541, 2017.

[110] G. Yildiz, F. Ronsse, R. Van Duren, and W. Prins, "Challenges in the design and operation of processes for catalytic fast pyrolysis of woody biomass," *Renew. Sustain. Energy Rev.*, vol. 57, pp. 1596–1610, 2016.

[111] ASTM, "Standard Test Method for Moisture Analysis of Particulate Wood Fuels 1," *Annu. B. ASTM Stand.*, vol. 82, no. Reapproved 2013, p. 2, 2014.

[112] ASTM International, "Standard Test Method for Volatile Matter in the Analysis Sample of Coal and Coke1 This," *Annu. B. ASTM Stand.*, vol. 03, no. February 2007, pp. 1–5, 2007.

[113] A. Wood, "Standard Test Method for," vol. 84, no. June 1984, pp. 1–2, 2001.

[114] J. Solar *et al.*, "Influence of temperature and residence time in the pyrolysis of

woody biomass waste in a continuous screw reactor," *Biomass and Bioenergy*, vol. 95, pp. 416–423, 2016.

[115] D. M. Marinković, J. M. Avramović, M. V. Stanković, O. S. Stamenković, D. M. Jovanović, and V. B. Veljković, "Synthesis and characterization of spherically-shaped CaO/Γ-Al2O3 catalyst and its application in biodiesel production," *Energy Convers. Manag.*, vol. 144, pp. 399–413, 2017.

[116] C. O. Osueke *et al.*, "Comparative calorific evaluation of biomass fuel and fossil fuel," *Int. J. Civ. Eng. Technol.*, vol. 9, no. 13, pp. 1576–1590, 2018.

[117] J. Ge, R. Q. Wang, and L. Liu, "Study on the Thermal Degradation Kinetics of the Common Wooden Boards," *Procedia Eng.*, vol. 135, pp. 72–82, 2016.

[118] J. L. Solis, L. Alejo, and Y. Kiros, "Synthesis and Catalysis of Mixed Oxides on Mesoporous Mayenite for Biodiesel Production from Castor Oil (Ricinus communis)," *Synth. Catal. Open Access*, vol. 03, no. 02, pp. 1–14, 2018.

[119] A. Lunguleasa, C. Spirchez, and O. Zeleniuc, "Evaluation of the calorific values of wastes from some tropical wood species," *Maderas Cienc. y Tecnol.*, vol. 22, no. 3, pp. 269–280, 2020.

[120] A. A. D. Maia and L. C. de Morais, "Kinetic parameters of red pepper waste as biomass to solid biofuel," *Bioresour. Technol.*, vol. 204, pp. 157–163, 2016.

[121] P. Parthasarathy and S. K. Narayanan, "Effect of Hydrothermal Carbonization Reaction Parameters on," *Environ. Prog. Sustain. Energy*, vol. 33, no. 3, pp. 676–680, 2014.

[122] D. Skoog, D. West, J. Holler, and S. Crouch, "Fundamentals of analytic chemistry," *Brooks/Cole*, p. 1088, 2014.

[123] P. Álvarez-Álvarez *et al.*, "Evaluation of tree species for biomass energy production in Northwest Spain," *Forests*, vol. 9, no. 4, pp. 1–15, 2018.

[124] A. I. Anukam, B. P. Goso, O. O. Okoh, and S. N. Mamphweli, "Studies on Characterization of Corn Cob for Application in a Gasification Process for Energy Production," vol. 2017, 2017.

[125] U. The and A. Autonomy, "Synthesis and Application of γ -Alumina Nanopowders By Shuchismita Dey," National Institute of Technology Rourkela.

[126] S. G. Bawa, A. S. Ahmed, and P. C. Okonkwo, "Alumina phase transformation from thermal decomposition of ammonium alum synthesized from kankara kaolin," *Niger. J. Technol.*, vol. 36, no. 3, pp. 822–828, 2017.

[127] M. R. Karim, "Synthesis of β-Alumina Particles and Surface Characterization,"

Open Colloid Sci. J., vol. 4, no. 1, pp. 32–36, 2011.

[128] I. Reyero, G. Arzamendi, and L. M. Gandía, "Heterogenization of the biodiesel synthesis catalysis: CaO and novel calcium compounds as transesterification catalysts," *Chem. Eng. Res. Des.*, vol. 92, no. 8, pp. 1519–1530, 2014.

[129] G. Busca, V. Lorenzelli, G. Ramis, and R. J. Willey, "Surface Sites on Spinel-Type and Corundum-Type Metal Oxide Powders," *Langmuir*, vol. 9, no. 6, pp. 1492–1499, 1993.

[130] Z. Zeng, J. Yu, and Z. X. Guo, "Preparation of functionalized core-shell alumina/polystyrene composite nanoparticles, 1 encapsulation of alumina via emulsion polymerization," *Macromol. Chem. Phys.*, vol. 206, no. 15, pp. 1558–1567, 2005.

[131] S. Ali, Y. Abbas, Z. Zuhra, and I. S. Butler, "Correction: Synthesis of γ-alumina (Al2O3) nanoparticles and their potential for use as an adsorbent in the removal of methylene blue dye from industrial wastewater (Nanoscale Adv., (2018) DOI: 10.1039/c8na00014j)," *Nanoscale Adv.*, vol. 1, no. 1, pp. 437–439, 2019.

[132] M. Galván-Ruiz, J. Hernández, L. Baños, J. Noriega-Montes, and M. E. Rodríguez-García, "Characterization of Calcium Carbonate, Calcium Oxide, and Calcium Hydroxide as Starting Point to the Improvement of Lime for Their Use in Construction," *J. Mater. Civ. Eng.*, vol. 21, no. 11, pp. 694–698, 2009.

[133] Y. H. Tan, M. O. Abdullah, C. Nolasco-Hipolito, and Y. H. Taufiq-Yap, "Waste ostrich- and chicken-eggshells as heterogeneous base catalyst for biodiesel production from used cooking oil: Catalyst characterization and biodiesel yield performance," *Appl. Energy*, vol. 160, pp. 58–70, 2015.

[134] N. Pasupulety, K. Gunda, Y. Liu, G. L. Rempel, and F. T. T. Ng, "Production of biodiesel from soybean oil on CaO/Al2O3 solid base catalysts," *Appl. Catal. A Gen.*, vol. 452, pp. 189–202, 2013.

[135] Y. Ding, O. A. Ezekoye, S. Lu, C. Wang, and R. Zhou, "Comparative pyrolysis behaviors and reaction mechanisms of hardwood and softwood," *Energy Convers. Manag.*, vol. 132, pp. 102–109, 2017.

[136] A. Aboulkas, K. El harfi, and A. El Bouadili, "Thermal degradation behaviors of polyethylene and polypropylene. Part I: Pyrolysis kinetics and mechanisms," *Energy Convers. Manag.*, vol. 51, no. 7, pp. 1363–1369, 2010.

[137] B. Dou, S. Park, S. Lim, T. U. Yu, and J. Hwang, "Pyrolysis characteristics of refuse derived fuel in a pilot-scale unit," *Energy and Fuels*, vol. 21, no. 6, pp. 3730–

3734, 2007.

[138] H. Hu, Q. Chen, Z. Yin, P. Zhang, J. Zou, and H. Che, “Study on the kinetics of thermal decomposition of mechanically activated pyrites,” *Thermochim. Acta*, vol. 389, no. 1–2, pp. 79–83, 2002.

[139] E. H. M. Diefallah, M. A. Gabal, A. A. El-Bellihi, and N. A. Eissa, “Nonisothermal decomposition of CdC2O4-FeC2O4 mixtures in air,” *Thermochim. Acta*, vol. 376, no. 1, pp. 43–50, 2001.

[140] C. Liu, H. Wang, A. M. Karim, J. Sun, and Y. Wang, “ChemInform Abstract: Catalytic Fast Pyrolysis of Lignocellulosic Biomass,” *ChemInform*, vol. 46, no. 3, p. no-no, 2015.

APPENDICES

Appendix A

Preparation of corn cob procedure

Corn cob

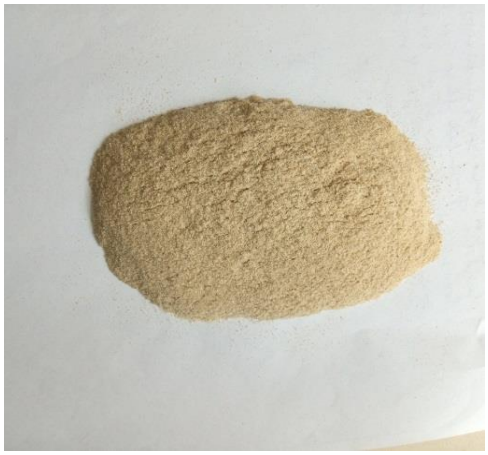

after size reduction

Heating value calculation

Table1:-Values of corrected temperature for the utilization of corn cob

Corn cob sample	Initial temperature(^oC)	Final temperature(^oC)	Difference in temperature(^oC)	Mass of sample
Trial 1	22.15	23.98	1.97	1.5698
Trial 2	22.10	24.13	2.03	1.623
Trial 3	22.89	25.12	2.05	1.554

Given

Mass of benzoic acid (m_{ba}) = 1.651 grams

Mass of Nichrome Fuse Wire (Mw) = 0.0184 gm.

Mass of Cotton Thread (Mt) = 0.005 gm.

Heat of combustion (q_{vba}) = 6318 cal/g

Rise in Temperature ΔT = 3.047°C

Capacity per Gram of Nichrome Fuse Wire (Hw) =333.68 Cal/gm

Heat Capacity per Gram of Cotton Thread (Ht) = 4180Cal/gm.

The Water Equivalent (ε) of the calorimeter is then calculated as follows:

$$Q_{fuse} = Mw*Hw = 0.0184 \text{ gm} * 333.68 \text{ Cal/gm} = 6.14 \text{ Cal}$$

$$Q_{ign} = Mt*Ht = 0.005 \text{ gm} * 4180 \text{ Cal/gm} = 20.9 \text{ Cal}$$

$$\varepsilon = \frac{m_{ba} * q_{vba} + Q_{fuse} + Q_{ign}}{\Delta T}$$

$$\varepsilon = \frac{1.651 * 6318 + 6.14 + 20.9}{3} = 3432 cal/°C$$

$$q_{CC} = \frac{\varepsilon * \Delta T - Q_{fuse} + Q_{ign}}{m_{CC}}$$

Table 2:-The calorific values of corn cob

Corn cob sample	Calorific value(Ca/g)
Trial 1	4290
Trial 2	4276
Trial 3	4510
Average	4358

Appendix B

Catalyst preparation procedures

Step2:- preparation of gamma alumina

a) Urea and alumina nitrate non-hydrates solution b) alumina gal

c) Amorphous gamma alumina

Step2:- preparation of calcium oxide with support gamma alumina

Calcium oxide with gamma alumna solution

Equipment used for characterization of catalyst

Fourier transforms infrared (FTIR)

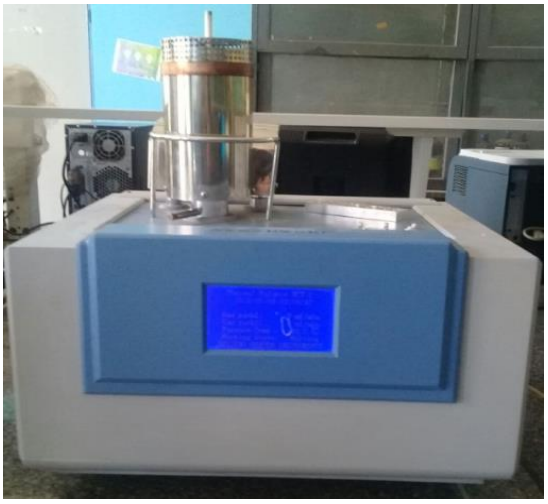

Thermogravimetry analysis (TGA)

Appendix C

Figure shows the Catalytic degradation of corn cob at different catalyst compositions (1, 3, 5, 7 and 10%CaO/γ-Al_2O_3).

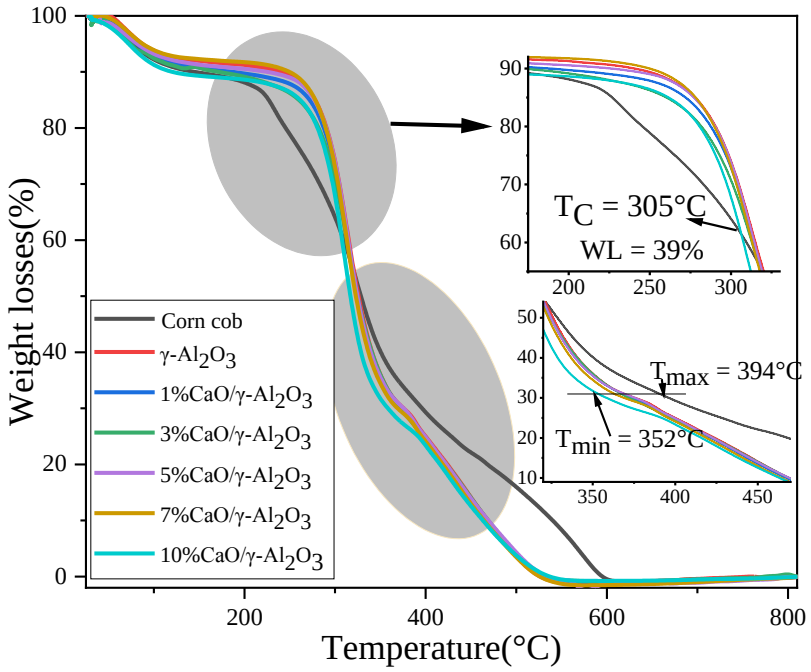

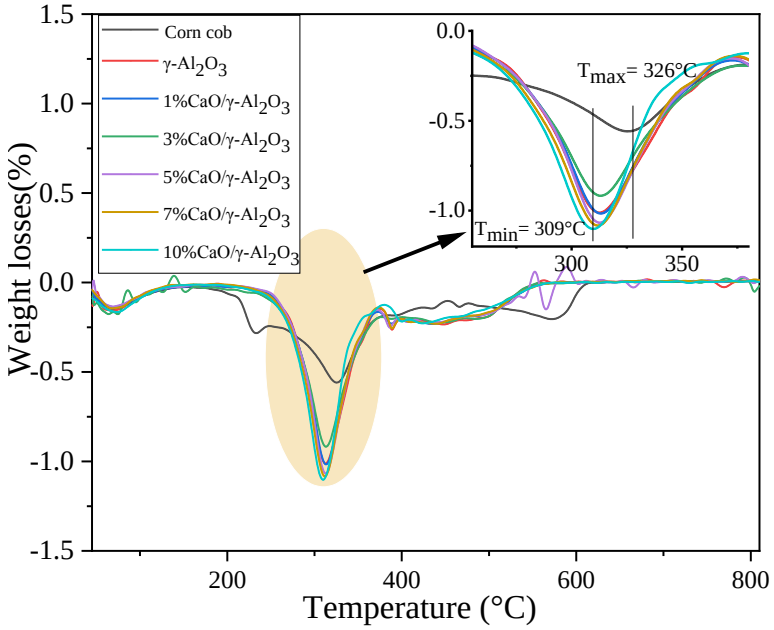

Table 3: - The kinetic parameters calculated using the model-fitting methods at four different heating rates.

Model	0.3-0.5							
	5 (^{o}C/min)	10 (^{o}C/min)	15 (^{o}C/min)	20 (^{o}C/min)	5 (^{o}C/mi	10 (^{o}C/min)	15(^{o}C/min)	20 (^{o}C/min)
F1	50.80584	42.05848	38.06583	37.01079	0.9991	0.9924	0.9977	0.962
F2	67.09149	56.24849	50.51391	49.23957	0.9994	0.9967	0.9938	0.9665
F3	85.89291	72.63893	64.8719	63.36079	0.9986	0.9986	0.9894	0.9683
F4	107.0038	91.0482	80.98539	79.21925	0.9972	0.9992	0.9852	0.9689
F5	130.1266	111.2145	98.63134	96.59103	0.9959	0.9992	0.9817	0.9689
F6	154.923	132.8404	117.5553	115.2213	0.9975	0.989	0.9989	0.961
F7	167.8429	144.1078	127.4168	124.9286	0.9946	0.999	0.9788	0.9688
D1	82.787	69.66686	62.86798	60.86515	0.9941	0.9989	0.9777	0.9685
D3	21.57986	16.69303	15.58614	15.12427	0.9934	0.9724	0.9644	0.9388
R2	43.63539	35.81415	32.57966	31.62786	0.998	0.9886	0.9988	0.9581
R3	46.00053	37.87352	34.3897	33.40328	0.9985	0.9901	0.9985	0.9596
P4	2.852296	0.484617	1.119314	1.128932	0.864	0.098	0.8454	0.79
P3	6.506454	5.582359	3.94211	3.85973	0.9649	0.9427	0.8679	0.8082
P2	14.27154	10.36779	9.940552	9.662677	0.989	0.954	0.986	0.9183
P2/3	59.94852	49.9005	45.2255	43.79766	0.9971	0.9873	0.9992	0.95825
A2	21.11944	16.32996	15.18195	14.80299	0.9977	0.9829	0.9975	0.9475
A3	11.02607	7.582263	7.401434	7.252336	0.9934	0.955	0.918	0.9153
A4	6.276248	3.4657	3.740014	3.699088	0.9814	0.8576	0.903	0.836
A2/3	31.21282	25.07766	22.96247	22.35364	0.9986	0.9888	0.9984	0.9561

Model	0.55-0.9							
	5 (^{o}C/min)	10 (^{o}C/ min)	15 (^{o}C/ min)	20 (^{o}C/min)	5 (^{o}C/min)	10 (^{o}C/min)	15 (^{o}C/min)	20 (^{o}C/min)
F1	17.22406	16.015	15.86801	15.86425	0.9991	0.9924	0.9977	0.962
F2	40.65672	39.74112	39.31475	38.76245	0.9994	0.9967	0.9938	0.9665
F3	71.33085	70.79586	69.99057	68.72231	0.9875	0.9854	0.97484	0.95757
F4	105.9758	105.8872	104.6687	102.5927	0.9865	0.9833	0.9753	0.9729
D1	15.33595	14.1133	14.07584	14.10148	0.9975	0.989	0.9989	0.961
D3	-1.31385	-2.79257	-2.79579	-2.35882	0.9934	0.9724	0.9644	0.9388
R2	8.964821	7.642247	7.57988	7.769914	0.998	0.9886	0.9988	0.9581
R3	11.51206	10.22559	10.13863	10.26885	0.9985	0.9901	0.9985	0.9596
P4	-6.40819	-7.96526	-7.958	-7.39519	0.864	0.098	0.8454	0.79
P3	-5.41417	-6.95595	-6.95074	-6.41248	0.9649	0.9427	0.8679	0.8082
P2	-3.30189	-4.81118	-4.81031	-4.32423	0.989	0.954	0.986	0.9183
P2/3	9.123336	7.805138	7.780459	7.959574	0.9971	0.9873	0.9992	0.95825
A2	3.854783	2.447834	2.381161	2.699056	0.9977	0.9829	0.9975	0.9475
A3	-0.69077	-2.165	-2.20437	-1.77711	0.9934	0.955	0.918	0.9153
A4	-2.82986	-4.33575	-4.36227	-3.88354	0.9814	0.8576	0.903	0.836
A2/3	8.68103	7.67274	7.332432	7.21491	0.9986	0.9888	0.9984	0.9561